

Advances in Spatial Omics Technologies

Tianxiao Hui, Jian Zhou, Muchen Yao, Yige Xie, and Hu Zeng*

Rapidly developing spatial omics technologies provide us with new approaches to deeply understanding the diversity and functions of cell types within organisms. Unlike traditional approaches, spatial omics technologies enable researchers to dissect the complex relationships between tissue structure and function at the cellular or even subcellular level. The application of spatial omics technologies provides new perspectives on key biological processes such as nervous system development, organ development, and tumor microenvironment. This review focuses on the advancements and strategies of spatial omics technologies, summarizes their applications in biomedical research, and highlights the power of spatial omics technologies in advancing the understanding of life sciences related to development and disease.

tissue context.^[2-4] This review aims to provide an overview of the latest advances in spatial omics technologies, highlighting their pivotal role in unraveling the intricate interplay between tissue architecture and cellular function. We further delve into the diverse applications of spatial omics technologies across various fields, including neurobiology, developmental biology, and cancer biology. The integration of spatial and molecular information provides a holistic view of cellular heterogeneity and dynamics, shedding light on fundamental biological processes such as nervous system development, organogenesis, and tumor

1. Introduction

In recent years, the advances of spatial omics technologies have revolutionized our ability to explore the intricate landscape of cellular diversity and functionality within organisms.^[1] These techniques have opened new avenues for researchers to delve into the complexities of biological systems at unprecedented resolution. By integrating spatial information with high-throughput omics approaches, such as transcriptomics, proteomics, genomics, epigenomics, and metabolomics, spatial omics technologies offer a comprehensive view of cellular activities within their

microenvironment dynamics.^[5-7] The applications of spatial omics technologies hold immense promise for advancing our understanding of complex biological phenomena and paving the way for innovative disease diagnosis and treatment approaches. This review highlights the significance of spatial omics technologies in driving forward the frontier of life sciences research and unlocking deeper insights into the complexities inherent in living organisms.

2. Current-Era Spatial Omics Technologies

Spatial technologies incorporate numerous high-throughput methods such as spatial transcriptomics, proteomics, translomics, genomics, epigenomics, and metabolomics to study the spatial distribution, interaction, and regulation of various biomolecules within biological systems.^[1] These holistic approaches allow researchers to gain a deeper understanding of the structure and function of biological systems, unveiling mechanisms underlying disease development, drug actions, and intricate regulatory networks within organisms. Spatial transcriptomics explores gene expression patterns and regulatory networks to understand the spatial organization of mRNA within cells or tissues.^[3] Spatial proteomics and translomics analyze protein expression levels, interactions, and the translation of mRNA into proteins, providing insights into the spatial distribution of proteins and their regulatory mechanisms.^[8] Spatial genomics and epigenomics investigate DNA's three-dimensional (3D) structure, chromatin organization, and the regulatory effects of epigenetic changes on gene expression, offering comprehensive insights into the spatial organization of the genome and its regulatory landscape.^[9,10] Metabolomics examines metabolite distribution and variation within cells or tissues, completing the spatial omics landscape by elucidating the spatial distribution and dynamics of cellular metabolites.^[11] By integrating these diverse layers of information, spatial omics technologies offer novel

T. Hui, H. Zeng
State Key Laboratory of Gene Function and Modulation Research
College of Future Technology
Peking-Tsinghua Center for Life Sciences
Peking University
Beijing 100871, China
E-mail: huzeng@pku.edu.cn

J. Zhou
Peking-Tsinghua Center for Life Sciences
Tsinghua University
Beijing 100084, China

M. Yao
College of Biological Sciences
China Agricultural University
Beijing 100193, China

Y. Xie
School of Nursing
Peking University
Beijing 100871, China

H. Zeng
Beijing Advanced Center of RNA Biology (BEACON)
Peking University
Beijing 100871, China

 The ORCID identification number(s) for the author(s) of this article can be found under <https://doi.org/10.1002/smt.202401171>

DOI: 10.1002/smt.202401171

perspectives and methodologies for understanding cellular function, disease mechanisms, and drug therapies.

2.1. Spatial Transcriptomics

2.1.1. NGS-Based Spatial Transcriptomics

A feasible way to spatially profile high-throughput transcriptome data involves integrating spatial information in the form of DNA barcodes into sequences during the standard library construction of single-cell RNA sequencing (scRNA-seq). There are two main categories of methods to achieve the addition of spatial barcodes to each mRNA transcript. One category uses the pre-treated microarrays with spatial barcodes to add spatial information when capturing mRNA transcripts. The other category involves incorporating spatial barcodes in situ before capturing transcripts.

Microarray-Based Spatial Transcriptomics: For NGS-based spatial technologies, the advanced and commercially viable strategies involve utilizing chips that carry spatial information in various forms, such as arrays, beads, colonies, or DNA nanoballs.^[12] The initial array example is spatial transcriptomics (ST) in 2016, featuring a resolution of 100 μm .^[13] In this study, Ståhl et al. immobilized oligo(dT) primers onto glass slides, and tissue was then placed over glass slides for permeabilization. Following cDNA synthesis via reverse transcription (RT), the sequencing libraries were generated through amplification in vitro transcription and subsequently processed using Illumina sequencing (Figure 1a). Moreover, ST was commercialized as the Visium platform by 10 \times Genomics, achieving a resolution of 55 μm . Recently, an enhanced version, the 10 \times Visium HD, has achieved single-cell resolution with an improved spot size of 2 $\mu\text{m} \times 2 \mu\text{m}$.

The bead-based microarray method, high-definition spatial transcriptomics (HDST), as an advanced version of ST, generates barcoded beads with a split-and-pool strategy and randomly places them into a hexagonal array of >1.4 million 2 μm wells to improve the spatial resolution (Figure 1a).^[14] A similar strategy named Slide-seq offers a 10 μm resolution and uses sequencing by oligonucleotide ligation and detection (SOLiD) for array generation and decoding.^[15] In the next version of Slide-seq, Slide-seqV2 adopts a monobase-encoding scheme with sequencing by ligation using sequential interrogation by offset primers and adds an additional second-strand synthesis step after RT to increase the number of cDNAs for optimization of library preparation.^[16] Moreover, Slide-tags, developed by the same authors, profiles tagged and isolated single nuclei analysis with spatial barcodes derived from DNA-barcoded beads with known positions to avoid cross-perturbation of transcripts from different cells in one spot.^[17] Techniques such as XYZeq^[18] and sci-Space^[19] share a similar purpose to dissociate the single cell or nuclei in spatially barcoded spots for downstream scRNA-seq, wherein two rounds of split-pool indexing and slide-specific oligo transferring with subsequent imaging are adopted, respectively.

As for strategies based on colonies, DNA nanoballs (DNB), and 3D dendrimeric slides, significant advantages include higher mRNA capturing efficiency and enhanced spatial resolution, which lead to a substantial increase in capturing efficiency per spot on 2D chips. A representative technology based on DNB is Stereo-seq,^[20] developed by Beijing Genomics Institution (BGI),

which uses 220 nm DNB spot arrays with 500 or 750 nm intervals between each spot and 10 mm \times 10 mm capturing area. During the Stereo-seq chip preparation, each DNB, assigned with random coordinate identities (CID), is sequenced to obtain spatial information of the chip and subsequently ligated with unique molecular identifiers (UMIs) and a poly(T) sequence by hybridization (Figure 1b). Finally, the 10 μm frozen tissue slides are placed onto chips followed by fixation and permeabilization to capture the poly(A)-tailed RNA. Two other approaches based on colonies or colonies, Seq-Scope^[21] and Pixel-seq,^[22] both utilize bridge amplification similar to Illumina sequencing and achieve nearly 1 μm resolution (Figure 1b). Particularly, compared to the decoding step for each chip using sequencing by synthesis (SBS) in Seq-Scope, Pixel-seq develops a “stamp-gel” strategy to copy spatially decoded gel templates from crosslinked polyacrylamide surface by DNA polymerase-catalyzed chain extension, significantly reducing the cost of chip-decoding steps (Figure 1b). Another method, called Decoder-seq, utilizes a microfluidic-based barcode-generating approach to simplify the decoding of data matrices on chips.^[23] In this study, Cao et al. adopted 3D dendrimeric arrays with multiple active primary amino groups on each spot, allowing the covalent crosslinking of high-density spatial DNA barcodes to increase mRNA capturing efficiency. With xy-orthogonal microfluidic channels, 5' amino-modified DNA barcodes are ligated onto chips by disuccinimidyl suberate (DSS) in the first round and combinatorial barcode sequences including UMIs and poly(T) tags are ligated in the second round through pre-hybridization with linker sequences.

Microfluidic-Based Spatial Transcriptomics: Instead of capturing RNA with pre-decoded spatial barcoding arrays, DBiT-seq^[24] tags the spatial barcodes onto tissue transcripts in situ using microfluidic devices. In this approach, a polydimethylsiloxane (PDMS) microfluidic chip containing 50 parallel microchannels with 10 mm in width is placed on the tissue slides twice in mutually orthogonal directions. The first round includes the hybridization of poly(T) primer and spatial barcodes with poly(A)-tailed mRNA transcripts followed by reverse transcription. The second round, utilizing a different flow direction, ligates DNA barcode B to the chip, incorporating a ligation linker, a distinct spatial barcode, a UMI sequence, and a PCR handle modified with biotin for subsequent cDNA purification using streptavidin beads (Figure 1c). After imaging the slide for morphology integration, the tissue can be dissected and cDNAs can be collected to prepare libraries. Moreover, DBiT-seq is also capable of spatially profiling proteins using DNA-conjugated antibodies. Further expansions for spatial multi-omics based on DBiT-seq will be discussed in the later section.

Spatial Transcriptomics based on Microdissection and Selective Illumination: A direct method for acquiring spatial information is using physical or optical marking to select regions of interest (ROI). Microdissection is a straightforward method for physically obtaining spatial molecular information, which includes Laser-capture microdissection (LCM),^[25] LCM-seq,^[26] and Tomoseq.^[27] LCM facilitates the precise microdissection of small areas or even single cells from frozen tissues (Figure 1d). For LCM, ROIs in the tissue section are dissected either by ultraviolet (UV) laser cutting or by fusion of tissue with a membrane using an IR laser. Recent versions of Arcturus combine these two techniques, with IR fusion facilitating the removal of the ROI that was

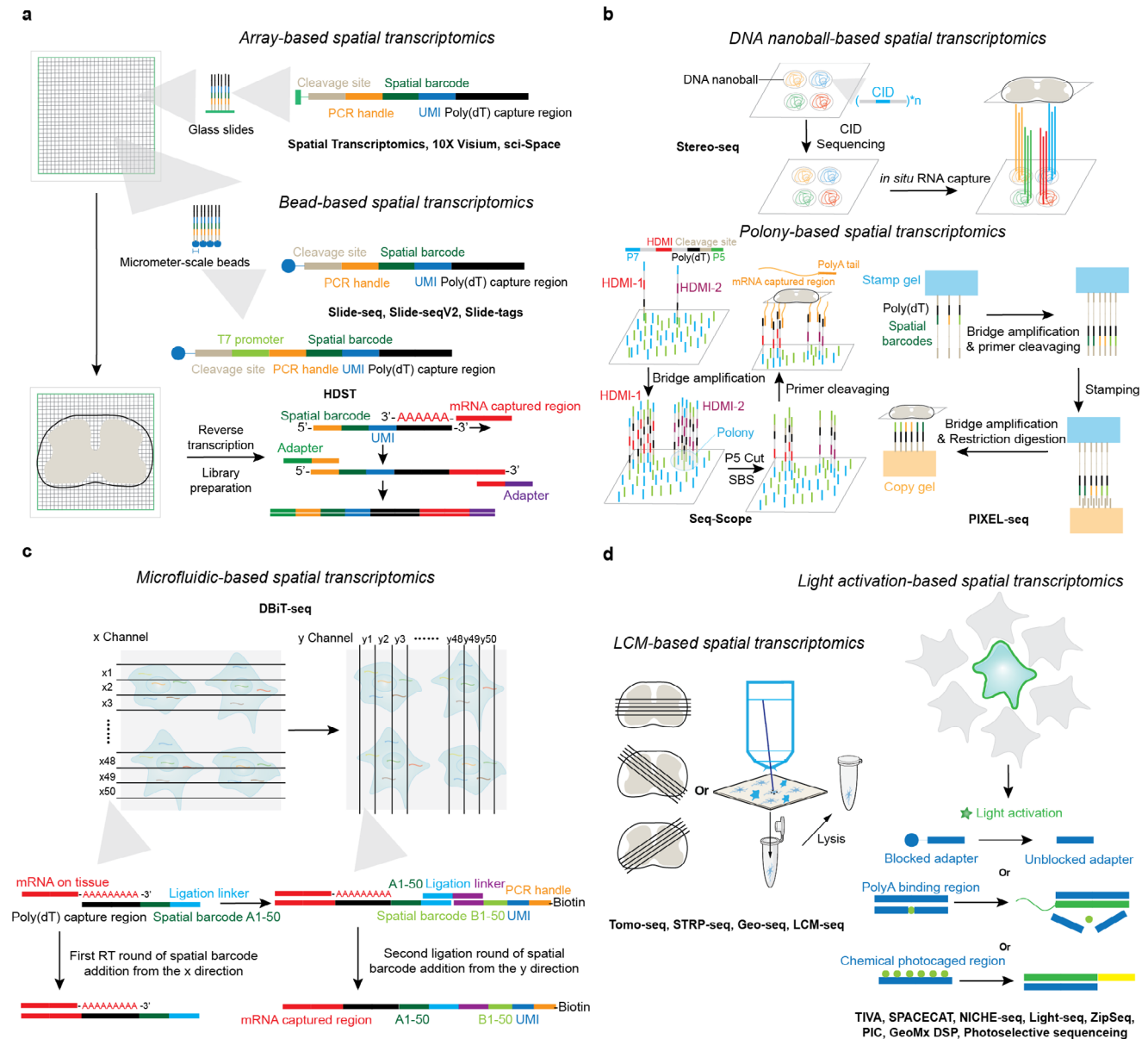


Figure 1. Schematics of next-generation sequencing-based spatial transcriptomics. a) Array-based and bead-based spatial transcriptomics using arrayed probes on the glass slide or beads to capture mRNA. b) DNA nanoball-based and polony-based spatial transcriptomics. Reproduced with permission.^[21] Copyright 2021, Elsevier. c) Microfluidic-based spatial transcriptomics by in situ ligation of the spatial barcodes. d) LCM-based and light activation-based spatial transcriptomics in a direct way to choose the region of interest.

previously cut using UV. Geographical position sequencing (Geo-seq)^[28] combines LCM with scRNA-seq to generate a 3D transcriptome atlas. More recently, an innovative microdissection approach called STRP-seq has been developed using a compressed sensing tissue sampling strategy based on multi-angle sectioning and an associated algorithm that enables the reconstruction of complex two-dimensional (2D) spatial patterns.^[29] However, microdissection methods are limited by low throughput profiling, which results in excessive time consumption.

Concerning optical marking strategies, light can be used to mark specific cells of interest or to directly label RNAs within the ROI. Based on photocaging, NICHE-seq^[30] and SPACECAT^[31]

adopt photoactivatable fluorophores for tagging, tracking, and isolating live cells (Figure 1d). Conversely, ZipSeq attaches anchor oligonucleotides with photocaged overhangs to cells in ROI using antibodies or lipid insertion followed by the addition of spatial “zipcodes” after photoactivation.^[32] Transcriptome in vivo analysis (TIVA)^[33] uses TIVA tags including disulfide-linked cell-penetrating peptide (CPP) for penetrating cell membranes and a photocleavable linker to block the detection probe modified with biotin targeting mRNA. In contrast, photo-isolation chemistry (PIC)^[34] employs photo-caged oligodeoxynucleotides (caged ODNs) to activate region-specific reverse transcription in response to light. Conversely, GeoMx Digital Spatial Profiling

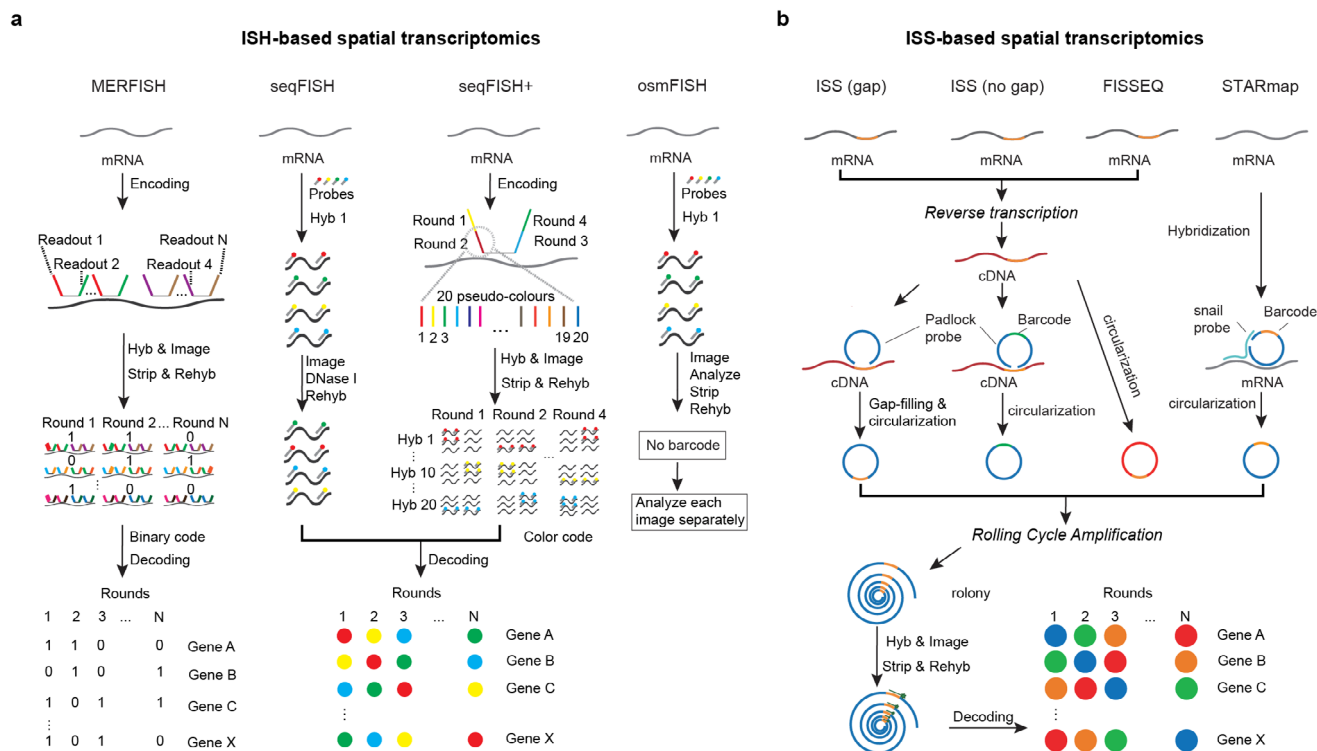


Figure 2. Schematics of image-based spatial transcriptomics. a) ISH-based spatial transcriptomics capture target RNA via in situ hybridization. b) ISS-based spatial transcriptomics capture transcripts information through rolling cycle amplification and in situ sequencing.

(DSP) profiles RNAs of interest using target oligonucleotides tagged with UV-photocleavable (PC) linkers, indexing oligonucleotides, and cleaving reporters with light.^[35]

A more recent approach named Light-seq utilizes the previously developed ultrafast photocrosslinker 3-cyanovinylcarbazole nucleoside (CNVK) to respond to UV light.^[36] In this method, Kishi et al. employ a degenerate primer for reverse transcription to label RNAs regardless of polyadenylation, resulting in the 3' ends of the synthesized cDNAs being polyA-tailed, which creates a 3' handle for ex situ primer binding. After CNVK and UMI-containing barcode strand hybridization and UV light photocrosslinking to the ROI, non-crosslinked barcode strands are washed away and barcoded cDNAs are collected from the sample following a mild RNase H treatment. Finally, a cross-junction synthesis reaction is performed to replicate both the barcoded DNA, and generated ssDNAs without crosslinking are prepared for NGS library preparation.

2.1.2. Image-Based Spatial Transcriptomics

In Situ Hybridization (ISH)^[37] and In Situ Sequencing (ISS)^[38] are imaging-based spatial transcriptomics techniques that enable the visualization and mapping of RNA molecules in intact tissue samples. ISH utilizes affinity probes that hybridize to target RNA sequences to provide spatial expression patterns of genes, whereas ISS typically involves the ligation of padlock probes or cDNA along with rolling circle amplification to label and identify RNA molecule through in situ sequencing. These methods provide insight into spatial gene expression patterns and contribute

to the understanding of cellular heterogeneity and organization in complex biological systems.

In Situ Hybridization-based Spatial Transcriptomics: In situ hybridization is a technique employed to quantitatively locate and detect nucleic acid molecules by hybridizing a labeled probe to the target nucleic acid sequences. This process is based on the complementary base pairing between the single strands.^[39] Traditionally, radioisotopes are used to label the probes, but due to the safety and instability of radioisotopes, fluorescence in situ hybridization (FISH) has emerged as a technique that uses fluorescence to label the probes. Femino et al. combined FISH with digital imaging microscopy to synthesize oligonucleotide probes with fluorescent dyes, which improved the ability of FISH to obtain quantitative molecular information on single cells and developed single-molecule fluorescence in situ hybridization (smFISH).^[40]

The Multiplexed Error-Robust Fluorescence In Situ Hybridization (MERFISH) technique was developed based on the single-molecule fluorescence in situ hybridization technique.^[41] MERFISH technology enables spatially resolved, highly multiplexed RNA analysis of formalin-fixed paraffin-embedded (FFPE) samples and fresh frozen samples at single-cell level. This technique utilizes fluorescent probes designed with error-robust combinatorial barcodes to hybridize RNA targets. Through sequential rounds of imaging and probe stripping, each RNA species is identified by decoding its unique barcode pattern, enabling spatial mapping at single-cell resolution (Figure 2a). In MERFISH, the probe consists of an mRNA-binding region and barcodes that can be detected by subsequent hybridization rounds. This

technique increases the number of genes imaged exponentially with the number of imaging rounds, significantly increasing the detection throughput.^[42] However, with an increase in the number of hybridization rounds, the RNA detection rate declined while the rate of RNA misidentification rose. To solve this problem, the MERFISH technique constructs an error correction strategy by utilizing modified Hamming codes so that each single-bit error can be detected and corrected, and double-bit errors can be recognized and discarded, which improves the accuracy of transcripts detection.

Sequential Fluorescence In Situ Hybridization (seqFISH) is a high-resolution multiplexed fluorescence in situ hybridization technique for spatial localization and quantification of RNA molecules at the cellular and tissue level.^[43] In seqFISH, a series of specific fluorescently labeled DNA probes are hybridized to target RNA sequences and then sequentially imaged, and after each round of imaging, the DNA probes are removed by DNase I treatment while the mRNAs are retained in situ to determine the spatial location and expression level of each RNA molecule. Each gene has a unique barcode, and probes of the same gene share the same barcode (Figure 2a). In each round of hybridization, every gene is associated with a specific color. The probe is removed to reveal the next color in the barcode, allowing for the subsequent round of hybridization. Therefore, utilizing four colors over eight rounds of hybridization ($4^8 = 65\,536$) is sufficient to encode all the genes within the human or mouse genome. Considering the potential for signal loss during hybridization, an additional round of error-correcting hybridization is necessary to ensure that the gene remains identifiable, even if the signal is lost in one of the rounds. Compared with traditional FISH technology, seqFISH has higher spatial resolution and multiplexing capability. It is capable of detecting multiple RNA species at the same time and enables high-throughput single-cell RNA localization and expression analysis. However, as sequencing throughput improves, the accuracy of high-precision in situ imaging may be constrained by optical resolution and the density of single-cell transcripts. In response, researchers developed an enhanced version called seqFISH+, building upon the original seqFISH technology.^[44] Using a standard confocal microscope, seqFISH+ technology is able to image mRNAs from 10000 genes in a single cell with high precision and sub-diffraction-limited resolution. The key to seqFISH+ is its extended barcode library (Figure 2a). While seqFISH uses four or five color dyes, seqFISH+ has a much larger set of “pseudo-colors”. In seqFISH+, it divides the 60 pseudo-colors into three fluorescent channels (Alexa Fluor 488, Cy3b, and Alexa Fluor 647) and generates barcodes only within each channel to avoid inter-channel color deviations. Using four rounds of imaging, each channel can accommodate up to 8000 barcoded genes with one round dedicated to error correction, and it is theoretically possible to detect up to 24 000 genes. By using 60 pseudo-color channels, the researchers effectively diluted the mRNA molecules into 60 separate images and positioned each mRNA spot below the diffraction limit before reorganizing the images to reconstruct a super-resolution image. Ouroboros smFISH (osmFISH) is a cyclic smFISH method that does not use a barcoding strategy but instead trades multiplexing capabilities for a simpler protocol that is not affected by transcript abundance or density (only a few transcripts are detected per cycle) (Figure 2a).^[45]

Although these FISH-based multiplexed methods have excellent sensitivity and transcriptome coverage at subcellular resolution, they suffer from rather long imaging times, which limit the size and thickness of the actual tissue. For example, in seqFISH+, when 80 rounds of hybridization/imaging were performed to detect 10000 transcripts, it took one week to image a single optical plane in a region of the cortical portion in a thin coronal tissue section of a mouse brain, despite the significant reduction of time compared to seqFISH. In addition to the difficulties of registration and barcode calling from these large raw image datasets, the resulting data suffers from the incompleteness of single-cell expression profiling because of the inability to perform unbiased detection of novel or variant minor sequences. Future initiatives should aim at developing rapid imaging protocols by implementing easy-to-use signal amplification. Simple and user-friendly interfaces for data acquisition and analysis in commercialization processes are essential to promote widespread use.

In Situ Sequencing-Based Spatial Transcriptomics: For in situ sequencing (ISS), a common step is the production of rolling circle amplification products (RCPs)—DNA “nanoballs” (rolony)—by performing rolling circle amplification (RCA) on circular templates generated from detected transcripts. Each mRNA molecule produces a separate colony, allowing for the quantification of transcripts.

ISS strategy originated from the technology developed by Ke et al.^[38] which allows RNA-seq to be performed directly on cells in primary tissues, providing a deeper understanding of gene expression of cells in relation to cell morphology and the local environment. In ISS, mRNA from intact tissue sections is first reverse-transcribed into cDNA, and then a specific padlock probe is designed to bind to it (Figure 2b). The end of the padlock probe is either precisely paired with the template and nicked for ligase to connect, or it is left with a gap that is filled by a polymerase before being nicked for ligase connection. Then the nucleic acid information in the target region is amplified by the method of rolling circle amplification, which generates the roll-around products, and finally, the RCPs are decoded through sequencing by ligation (SBL) to detect and analyze individual mRNA molecules. The strategy of direct ligation of the padlock probe by ligase allows the reporter region to be placed in an unpaired region, but this requires a unique barcode to be set in advance for the target region of interest. The strategy of filling the gap by DNA polymerase and then ligating it by ligase allows the reading of any sequences present in the gap, i.e., non-targeted sequencing, which allows for gene expression profiling and contributes to the study of gene mutations. This technique is simple to perform and has a resolution up to the subcellular level, but its detection throughput is limited.

However, padlock probes can have probe-specific biases and the ISS method does not easily scale to the whole transcriptome, so Lee et al. further developed fluorescence in situ sequencing (FISSEQ).^[46] This technique allows for genuine “off-target” sequencing in space, but it comes with the drawback of ultimately very low sensitivity (well below 1% of total cellular transcripts) due to the low efficiency of in situ reverse transcription and cDNA ligation into a loop. FISSEQ uses labeled random hexamer primers in fixed cells to reverse transcribe RNA to cDNA, which is then rolled up and amplified, and finally the RCPs are

sequenced (Figure 2b). FISSEQ enables targeted in situ sequencing to shift to untargeted in situ sequencing, which increases the number of sequenced transcript products and allows genome-wide expression profiles to be obtained. However, this method is inefficient and difficult to implement in tissue samples. Barcode in situ targeted sequencing (BaristaSeq) improves efficiency by optimizing the gap-filling padlock probe method and using Illumina synthetic sequencing for detection.^[47]

Similarly, the spatially-resolved transcript amplicon readout mapping (STARmap) technology combines hydrogel histochemistry with in situ sequencing.^[48] It uses two probes and a novel two-base sequencing protocol to achieve single-cell measurements of more than 1000 genes in intact tissues (Figure 2b). STARmap analyzes intact tissue samples in three dimensions, but is only suitable for 100–150 µm thick cross-sections and for smaller numbers of samples. Gyllborg et al. improved the design of lock probes to create a new barcoding system and replaced SBL with sequencing by hybridization (SBH), an approach known as hybridization-based in situ sequencing (HybISS).^[49] The design of HybISS improves flexibility and signal-to-noise ratio for improved visualization of spatial transcripts. Alon et al. developed the expansion sequencing (Exseq)^[50] technology, which employs expansion microscopy (ExM)^[51] to physically extend biological samples. This approach enhances spatially accurate untargeted or targeted in situ RNA-seq, enabling highly multiplexed RNA-seq from the nanoscale to the systems level.

2.2. Spatial Omics beyond Transcriptomics

2.2.1. Spatial Proteomics and Translatomics

Spatial proteomics and translatomics technologies encompass advanced methodologies for mapping and analyzing protein distribution and expression within cells and tissues. Techniques like mass spectrometry-based spatial proteomics, Imaging Mass Cytometry (IMC), Multiplexed Ion Beam Imaging (MIBI), and antibody-based spatial proteomics leverage mass spectrometry, metal-tagged antibodies, and DNA-conjugated antibodies to attain high-resolution imaging and quantitative analysis of protein localization. Spatial translatomics methods like RIBOmap offer insights into protein expression by mapping ribosome-bound mRNAs at molecular resolution. These cutting-edge technologies revolutionize our understanding of protein function, interactions, and disease mechanisms, facilitating advancements in biomedical research and drug development.

MS-Based Spatial Proteomics: MS-based spatial proteomics technology utilizes mass spectrometry (MS) to qualitatively and quantitatively analyze proteins in samples.^[8] By combining high-resolution imaging with mass spectrometry analysis, it separates and identifies proteins from different spatial locations within a sample, providing information on the spatial distribution of proteins within tissues or cells (Figure 3a). This technology is significant for uncovering the functions and interactions of proteins in biological systems and is widely applied in biomedical research, drug development, and the study of disease mechanisms.^[52]

IMC combines Cytometry by Time-Of-Flight (CyTOF) mass cytometry with immunohistochemistry (IHC) and immunocytochemistry (ICC) techniques, using metal-tagged antibodies and high-resolution laser ablation to achieve subcellular res-

olution imaging of multiple proteins and their modifications simultaneously.^[53] Its workflow includes sample preparation (following standard IHC/ICC protocols), antibody metal tagging (using rare-earth metal isotopes), laser ablation and mass spectrometry analysis (detection of metal isotopes via the CyTOF mass cytometer), and data analysis (computational segmentation of single-cell features and extraction of marker expression data). IMC integrates spatial information through the combination of high-resolution laser ablation and CyTOF mass spectrometry, where the signal from each laser ablation point is recorded and reconstructed into high-dimensional images, achieving spatial distribution imaging of proteins within tissues.^[54]

MIBI uses secondary ion mass spectrometry to image antibodies labeled with metal isotopes, allowing for the simultaneous detection of multiple markers with high sensitivity and resolution, suitable for standard FFPE tissue sections.^[55] Its workflow includes sample preparation (immobilizing samples on a conductive substrate), staining with metal-conjugated antibodies, ion beam analysis (scanning the sample surface with an ion beam to sputter isotopes), and data analysis (image segmentation and classification to generate composite images). MIBI integrates spatial information through secondary ion mass spectrometry, where the sample surface is scanned with an oxygen primary ion beam that sputter antibody-specific isotopes as secondary ions. Image segmentation is used to extract cellular features, and then quantitative and categorical analyses generate composite images that reveal the spatial characteristics of protein expression and intracellular distribution.^[56]

Antibody-Based Spatial Proteomics: Multiplexed antibody-based spatial proteomics can be categorized into fluorophore-labeled methods and DNA barcode-labeled methods. Although fluorophore-based proteomics technologies were initially established and have developed over decades alongside IF technologies, the limited number of channels and antigen usage per imaging cycle compel researchers to undertake iterative and multi-step processes. These processes consume much time for antibody incubation and carry the risk of epitope loss and incomplete fluorophore inactivation across successive cycles.^[57] For example, techniques such as MACSima Imaging Cyclic Staining (MICS),^[58] multi-epitope-ligand cartography (MELC),^[59] cyclic immunofluorescence (CycIF),^[60] and Multiplex Immunohistochemistry (Multiplex IHC)^[61] for FFPE tissues all adopt cyclic steps of antibody incubation and dissociation for imaging.

More applicable and extensive spatial proteomics technologies for high-throughput multiplex imaging are based on DNA-conjugated antibodies. Cellular indexing of transcriptomes and epitopes by sequencing (CITE-seq)^[62] is a representative method for co-profiling proteins and RNAs at a single-cell level. This is accomplished by the conjugated DNA design, featuring epitope-specific barcodes and a polyA sequence for simultaneous sequencing with RNA. GeoMx DSP^[35] also employs NGS assisted with microcapillary as the final step, although it requires selecting ROI for region-specific UV-dependent cleavage to obtain oligos from antibodies (Figure 3a).

Co-detection by indexing (CODEX)^[63] adopts sequential primer extension with in situ polymerization-based indexing, featuring a 15-cycle staining pattern that demonstrates cycle-specific signals, low background, efficient fluorophore release via inter-cycle TCEP (Tris(2-carboxyethyl) phosphine hydrochloride)

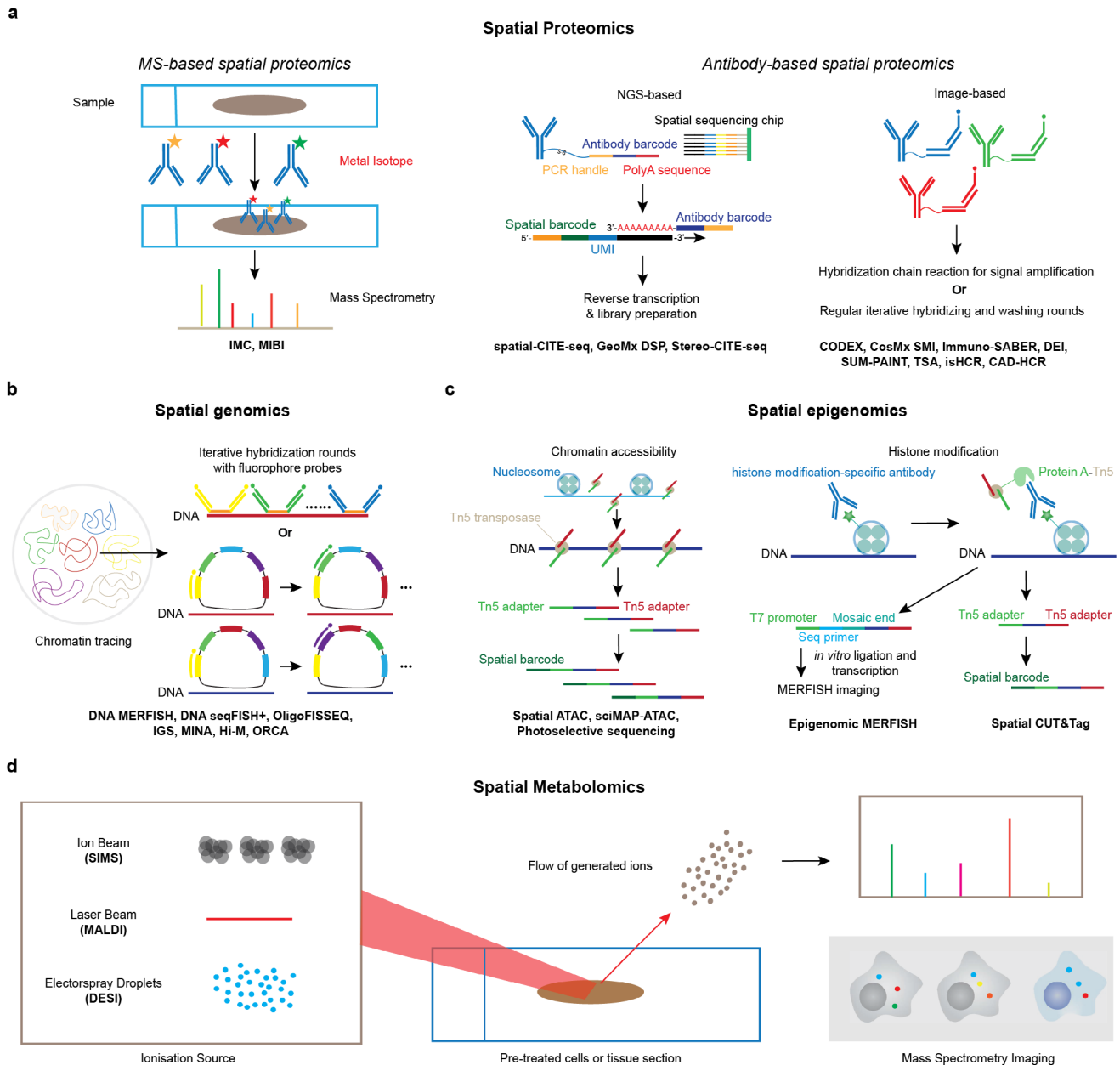


Figure 3. Schematics of spatial omics technologies beyond transcriptomics. a) MS-based and antibody-based spatial proteomics using antibody-conjugated metal isotopes, fluorophores and DNA splints. b) Spatial genomics focusing on chromatin tracing using imaging-based techniques. c) Spatial epigenomics, chromatin accessibility, and histone modifications mapped using the protein A-Tn5 transposase for the ligation of barcodes or adapters. d) Spatial metabolomics using ion beams, laser beams, or electrospray droplets to perform mass spectrometry imaging analysis of pre-treated samples.

cleavage and no signal carryover between cycles (Figure 3a).^[64] Moreover, FFPE-CODEX^[65] has been developed and optimized for clinical FFPE samples from colorectal cancer patients, enabling subsequent analysis of the tumor microenvironment. Building on the previously developed Exchange-PAINT,^[66] DNA Exchange Imaging (DEI)^[67] can be generalized to other super-resolution microscopy systems. Similarly, a more recent spatial proteomic approach called SUM-PAINT^[68] achieves single-protein resolution using a primary barcode for DNA-PAINT and a secondary label including a speed-optimized docking sequence

and a 10-nt toehold for gentle signal extinction via toehold-mediated strand displacement.

However, the methods mentioned above, employing various imaging strategies, lack signal amplification for a higher signal-to-noise ratio. In previous amplification strategies, tyramide signal amplification (TSA)^[69] based on the ability of horseradish-peroxidase (HRP) to catalyze the tyramide around the protein-antibody complex lacks orthogonal channels. Meanwhile, RCA acting on a circular template to synthesize long concatenated repeats cannot control the spatial resolution for individual targets.

The hybridization chain reaction (HCR)^[70] utilizes the triggered assembly of metastable fluorescent conjugated hairpins to generate tethered fluorescent amplification polymers and is compatible with antibody-based proteomics, including immuno signal HCR (isHCR)^[71] and computer-aided design of reversible HCR (CAD-HCR).^[72] Specifically, CAD-HCR develops a computer-aided approach to build a sequence database that enables the construction of multiple independent and simultaneous HCRs.

Besides the HCR approach, CosMx spatial molecular imager (SMI), developed by NanoString, relies on ISH probes and branching fluorescent readout probes known as reporters.^[73] These reporters contain between 15 and 60 dyes to adjust the signal amplification and are assembled with fluorophore-conjugated oligos as photocleavable (PC) linkers. Additionally, Immunostaining with signal amplification by exchange reaction (Immuno-SABER) achieves simultaneous signal amplification for proteins, extending beyond spectral multiplexing.^[74] In this method, orthogonal single-stranded DNA concatemers, generated by primer exchange reactions (PERs), are added following DNA-tagged antibody incubation for concatemer hybridization and further hybridized with fluorescent imagers. Furthermore, Immuno-SABER can be integrated with iterative branching design and Expansion Microscopy for enhanced sensitivity, resolution, and efficiency, ultimately reaching 5- to 180-fold signal amplification in various samples such as cultured cells and FFPE tissue samples.

Recently, Molecular Pixelation (MPX), a novel method developed by Pixelgen, employs a two-round pixelation strategy adding spatial barcodes through gap-fill ligation onto DNA-tagged antibody-oligonucleotide conjugates (AOCs) bound to target proteins in local neighborhoods on fixed cells.^[75] This approach facilitates a high-resolution mapping of protein distributions at the subcellular level, enabling precise spatial proteomics analysis based on NGS.

Spatial Translatomics: Besides direct protein spatial profiling, translatomics serves as a bridge between transcriptomics and proteomics, revealing the regulations at the translation level and providing a better correlation with actual protein expressions superior to that of transcriptomics alone. Previous approaches such as single-cell Ribo-seq (scRibo-seq)^[76] can achieve single-cell and single-codon resolution, albeit at the expense of spatial information. Ribosome-bound mRNA mapping (RIBOmap)^[77] adopts a tri-probes design strategy to selectively detect ribosome-bound mRNAs and amplify the signals via RCA. In this method, splint DNA probes that hybridize with ribosomal RNAs (rRNAs) act as templates for nick ligation, circularizing the adjacent padlock probes as RCA templates. A primer probe serves as a primer for RCA to produce DNA amplicon. The gene-unique barcodes in the DNA amplicon are readable through SEDAL sequencing, similar to STARmap.

2.2.2. Spatial Genomics and Epigenomics

Spatial Genomics: Compared to 3D genomics, which focuses only on an intranuclear level, spatial genomics seeks to profile 3D architecture variations of nuclei in multicellular samples such as tissues or organs. At the initial stage, multiplexed oligo-based FISH can be utilized to reconstruct the trajectory of long stretches of DNA, known as chromatin tracing, which includes methods

like super-resolution chromatin tracing, OligoDNA-PAINT, and OligoSTORM.^[78,79] As the first chromatin tracing method, super-resolution chromatin tracing reaches a resolution of 1–4 Mb, comparable to the resolution of a simple Hi-C experiment.^[80] Subsequently, oligopaint probes were utilized in conjunction with STORM (stochastic optical reconstruction microscopy) to trace TAD (topologically associating domain)-resolved organization in 1.2–2.5 Mb regions at a kilobase resolution.^[81] Moreover, image-based methods such as Hi-M^[82] and ORCA^[83] combine RNA FISH and Hi-C data to analyze 22 DNA loci at 17 kb resolution alongside one target RNA and 70 DNA loci at 10 kb and 52 loci at 2 kb alongside 29 different RNAs respectively for profiling embryo-scale samples.

Image-based spatial transcriptomics techniques such as MER-FISH, seqFISH+, and FISSEQ, can expand their applications from RNA FISH to DNA FISH. For multimodal imaging on mammalian tissues, the Multiplexed Imaging of Nucleome Architectures (MINA) method takes the initial step by combining multiscale chromatin tracing, achieving 50 DNA loci at 1 Mb and 19 DNA loci at 5 kb resolution, along chromosome 19 with 137 RNA MERFISH targets.^[84] Moving forward to DNA MERFISH^[85] and DNA seqFISH+^[86] the number of DNA loci for multiplexed FISH per cell has increased to hundreds and thousands (Figure 3b). However, since both methods adopt a combinatorial barcoding strategy at each locus with non-unique signals, sequential hybridization becomes essential to avoid spatial overlap and enhance genome resolution for TAD organization. OligoFISSEQ, as a combination of Oligopaints with FISSEQ, employs multiple sequencing strategies that decode Oligopaints through ligation, synthesis, and hybridization-based interrogation of targets.^[87] To notice, these spatial genomic methods are also compatible with IF for profiling proteins that construct nuclear structures simultaneously.

There are also methods combining image-based and NGS-based technologies for profiling spatial genomics. In situ genome sequencing (IGS) uses adapter ligation by Tn5 transposases and circularization for in situ RCA, followed by ISS, ex situ UMI, gDNA sequencing, and computational integration of these readouts.^[88] In Slide-DNA-seq,^[9] microarrays with 10 μm pixel sizes are used to ligate photocleavable spatial barcodes from beads to proximal genomic fragments, which are pretreated with HCl and Tn5 transposases before being collected for DNA NGS library construction. Although Slide-DNA-seq lacks subcellular resolution, its integration with Slide-RNA-seq facilitates the analysis of transcriptional programs driven by genetic aberrations and tumor density.

Spatial Epigenomics and Epitranscriptomics: Besides 3D nucleosome organization, there are also spatial epigenetic features including chromatin accessibility, histone modifications, and RNA modifications. The assay for transposase-accessible chromatin using sequencing (ATAC-seq)^[89] has been developed using DNA fragmentation by Tn5 transposase-induced adapter addition, which has been further applied to single cells.^[90] ATAC-seq^[91] also confirms the possibility of profiling chromatin accessibility in situ. Recently, various ATAC-seq methods with spatial resolutions, such as sciMAP-ATAC,^[92] spatial ATAC,^[93] Spatial-ATAC-seq^[94] and Photoselective sequencing^[95] have been developed based on LCM, ST, DBiT-seq, and optical marking,

respectively, which mostly adopt NGS-based spatial transcriptomics (Figure 3c).

As for profiling histone modifications, the recently developed image-based Epigenomic MERFISH^[10] and NGS-based Spatial-CUT&Tag^[96] use protein A fused with transposase Tn5 (pA-Tn5) and antibodies against various target histone modifications to ligate loaders or adapters to DNA segments for next sequencing steps, which are based on cleavage under targets and tagmentation (CUT&Tag) mechanism (Figure 3c). These methods demonstrated that active promoters and putative enhancers at the tissue level, along with subnuclear structures like speckles at the cellular level, are spatially and functionally associated with histone modifications such as H3K27me3, H3K4me3, and H3K27ac. Moreover, a spatial epigenomic tomography approach dissects mouse neocortex in layer-by-layer slices to obtain sufficient neurons and glia for microfluidic oscillatory washing-based chromatin immunoprecipitation followed by sequencing (MOWChIP-seq).^[97,98]

Compared to epigenomics, epitranscriptomics for RNA modification profiling remains a challenge moving forward to a spatial stage. There are only a few non-multiplexed methods capable of achieving spatial resolution. The m⁶A-specific in situ hybridization mediated proximity ligation assay (m⁶AISH-PLA) uses a proximity ligation strategy to detect HSP70 mRNA m⁶A site at a single-cell level.^[99] Here, proximity probe-b binds to m⁶A antibody and proximity probe-a binds to the target RNA, facilitating the formation of complete circular RCA template. Moreover, sialic acid aptamer and RNA in situ hybridization-mediated proximity ligation assay (ARPLA) for profiling glycosylated RNAs.^[100] In the ARPLA approach, dual recognition occurs in proximity with the twice nick-ligation of future circular RCA templates accomplished by the glycan probe, which includes a sialic acid aptamer and linker G, and the RNA-binding probe including RNA target sequence and linker R.

2.2.3. Spatial Metabolomics

Single-cell spatial metabolomics is a cutting-edge technology that offers a new avenue for understanding cellular metabolic activities by integrating single-cell analysis and spatial imaging techniques.^[101] This approach not only allows for the investigation of metabolic characteristics of individual cells but also enables the exploration of spatial relationships both between and within cells. By combining the relative positions of single cells with their metabolomic features, spatial metabolomics technology provides researchers with a unique opportunity to study cellular communication and interactions.^[102] However, this field faces challenges such as handling small volumes of materials during sample processing and transfer, as well as the high sensitivity requirements for metabolite detection. Despite these challenges, the emergence of new technologies like mass spectrometry imaging (MSI),^[103] selective cell sampling (SCS), and three-dimensional spatially resolved metabolomic profiling framework (3D-SMF)^[104] provides important tools and insights for gaining a deeper understanding of single-cell metabolic activities.

Mass Spectrometry Imaging (MSI): There are three major MSI approaches: secondary ion mass spectrometry (SIMS);^[105]

matrix-assisted laser desorption ionization (MALDI);^[106] and desorption electrospray ionization (DESI)^[107] (Figure 3d).

SIMS^[105] utilizes a focused ion beam to sputter secondary ions from the surface of the sample, which are then analyzed by a mass spectrometer. This technique offers the highest spatial resolution among MSI methods, with NanoSIMS achieving resolutions down to 50 nm for elemental ions.^[108,109] The typical workflow for SIMS involves preparing samples by freeze-drying or freeze-hydrating to prevent cell lysis. Cells can be grown on substrates or prepared as tissues. During ion beam sputtering, focused ion beams (such as bismuth or argon clusters) are used to eject secondary ions from the sample surface. These ions are subsequently analyzed by a high-resolution mass spectrometer. SIMS and its extended technologies like time-of-flight secondary ion mass spectrometry (TOF-SIMS)^[110] are widely applied in metabolite profiling, providing broad coverage of metabolites including lipids, amino acids, and sugars. It is also employed for cell type identification, such as classifying macrophage subtypes, and for identifying metabolic pathways. Moreover, SIMS facilitates single-cell multi-omics by combining metabolomics data with other omics datasets for comprehensive cellular analysis. Despite its high spatial resolution, SIMS faces challenges like ion fragmentation, which can complicate metabolite identification, and generally lower throughput compared to other MSI techniques.

MALDI^[111] employs a laser to ionize samples embedded in an organic matrix, which absorbs the laser energy and protects the analytes from fragmentation, resulting in the liberation of a greater proportion of intact molecules compared to SIMS. The workflow involves fixing cells or tissues and embedding them in the matrix, with potential staining to correlate cell types with metabolite profiles. The laser then ablates the matrix, causing desorption and ionization of the analytes, which are subsequently analyzed by a mass spectrometer to generate spatially resolved metabolite profiles.^[112] MALDI allows for sub-cellular resolution visualization and is used for lipid fingerprinting of different cell types, such as neurons and astrocytes, and for classifying cancer cell lines and understanding lipid roles in cell state determination.^[113,114]

DESI^[115] utilizes ambient ionization to analyze samples in their native state using a spray of charged solvent droplets. It typically has lower spatial resolution compared to SIMS and MALDI, though nano-DESI shows improved performance. The workflow involves minimal sample preparation, as DESI can analyze samples directly on surfaces like glass slides. A charged solvent spray is directed at the sample surface, causing desorption and ionization of the analytes, which are then analyzed by a mass spectrometer to produce metabolite images.^[107] DESI is suitable for ambient analysis, allowing the profiling of metabolites in various biological samples, without extensive preparation.^[116]

Selective Cell Sampling (SCS): SCS^[11] revolutionizes cellular analysis through its core techniques and key steps. Utilizing nanocapillaries or nano-spray emitters, SCS enables the precise collection of individual living cells under microscopic observation. Decoupling cell sampling from ionization allows for the manipulation of extracted materials before mass spectrometry analysis, enhancing versatility and accuracy. The workflow entails the selection and collection of cells, followed by lysis, solvent addition, ionization, and direct analysis via nano-electrospray

ionization. Enhanced sensitivity is achieved through techniques like chromatographic separation and chemical derivatization during data processing. SCS finds applications in diverse fields, including drug penetration studies, where it enables the measurement of drug interaction and penetration within single living cells. Moreover, it facilitates investigations into cell-cell interactions, shedding light on cellular responses to stimuli and mechanisms of drug resistance. Additionally, SCS enables sub-cellular analysis by sampling specific compartments to study metabolic processes within organelles. This innovative approach holds immense promise for advancing cellular research and deepening our understanding of complex biological systems.

Three-Dimensional Spatially Resolved Metabolomic Profiling Framework (3D-SMF): 3D-SMF^[104] utilizes TOF-SIMS to conduct spatial metabolite analysis of specific anatomical regions in tonsil samples. TOF-SIMS subjected FFPE tonsil tissue slices to repeated sputtering cycles with a cesium ion gun to remove the oxidized/intermediate layer. Subsequently, analysis was performed with a bismuth ion gun to generate secondary ions, measuring 50 to 150-depth images stacked to produce high-resolution chemical maps and three-dimensional chemical reconstructions. This approach is complemented by the incorporation of labeling techniques from CyTOF and IMC, using a library of 20 isotope-tagged antibodies for tissue staining and subsequent TOF-SIMS measurements to correlate specific cell features with metabolites. 3D-SMF enables analysis of volumetric metabolic fragment maps and cell features of immune cells in different anatomical regions of tonsils, providing a novel tool for a deeper understanding of metabolic activities and cell-specific features within tonsil structure.

2.3. Spatial Multi-Omics

Multimodal analysis within the same sample has become increasingly important for creating a molecular landscape that reflects multiple regulatory layers of the central dogma, applicable not only at the single-cell level but also across spatial multicellular tissue levels. Besides computational integration of multi-omics with data from previous studies or the collection of adjacent slides, simultaneous spatial omics profiling can generate more specific and accurate correlation analysis avoiding batch effects and other subtle factors.

2.3.1. Spatial (Epi) Genomics Plus Transcriptomics

In principle, nucleic acids hybridization and barcode ligation are universally applicable to both DNA and RNA. Therefore, as mentioned, spatial genomics can naturally integrate RNA FISH with DNA FISH as demonstrated by DNA MERFISH and DNA seqFISH+. SABER-FISH^[117] harnesses the programmability, orthogonality, and simplicity of PER to enhance the functionality of oligonucleotide-based FISH probes for both DNA and RNA targets. Spatial ATAC-RNA-seq and Spatial CUT&Tag-RNA-seq^[7] as representatives for spatial epigenomic methods, also enable separate and combined cell type classification, aiding in the identification of newly multimodal defined cell clusters. Another microfluidic-based spatial approach called microfluidic indexing-based spatial assay for transposase-accessible chromatin and

RNA-sequencing (MISAR-seq)^[118] can achieve similar goals for co-profiling gene expression and chromatin accessibility or histone modifications.

2.3.2. Spatial Transcriptomics Plus Proteomics

Two spatial multi-omics developed and commercialized by NanoString, GeoMx DSP and CosMx SMI, which have been previously described, can profile both spatial proteomics and transcriptomics simultaneously on FFPE samples.^[35,73] Similar to the NGS-based GeoMx DSP, there are other microarray-based methods co-profiling proteomics and transcriptomics for uniform library preparation and achieving whole-transcriptome coverage. Spatial-CITE-seq, based on DBiT-seq, utilizes microfluidic devices to integrate spatial barcode and capture cDNA and adapter-ligated antibody-derived DNA tags (ADTs).^[119] Similarly, Spatial Protein and Transcriptome Sequencing (SPOTS)^[120] and Spatial Multi-Omics (SM-Omics)^[121] both capture RNAs and ADTs using oligo(dT)-incubated arrays with spatial barcodes like Visium for subsequent library preparation. SM-Omics has also been developed as a high through-put and automated platform.^[121] For spatial transcriptomics using arrays based on DNB, Stereo-seq from BGI has also advanced to combine with CITE-seq, generating Stereo-CITE-seq that similarly co-captures RNAs and ADTs.^[122] Besides NGS-based technologies, there are also imaging-based spatial multi-omics technologies that enable co-mapping of spatial transcriptomics and protein signals.^[123,124] STARmap with protein localization and unlimited sequencing (STARmap PLUS) uses antibody staining and chemical labeling to simultaneously map spatial transcriptomics and disease marker proteins.^[123] Multi-omics in situ pair-wise sequencing (MiP-seq) designs primer and padlock probes targeting ADTs for downstream RCA and dual-barcode sequencing, achieving spatially simultaneous detection of DNA, RNA, proteins, and other biomolecules like neurotransmitters.^[124]

While GeoMx DSP utilizes an optical selection strategy with limited resolutions, CosMx SMI achieves subcellular resolution through the use of in situ hybridization probes and reporter amplifications.^[73] An analogous method, termed Multi Omic Single-scan Assay with Integrated Combinatorial Analysis (MOSAICA),^[125] also opts to design primary hybridization probes and double-ended secondary probes with fluorophores on each end for in situ imaging. However, it utilizes lifetime imaging with fit-free phasor analysis and combinatorial encoding with error-correction cycles.

3. Applications of Spatial Omics

3.1. Spatial Omics in Neurobiology

Mammalian neural systems display remarkable diversity in brain cell types as well as in their functional architectures, topographies, and connectivity.^[126] The brain contains billions of cells that form intricate interaction networks with specific spatial distribution patterns. Understanding such a complex organ requires mapping the molecular signatures of brain cell atlas, not only across the entire landscape (Figure 4a) but also within specific regions and functional cells participating in neural circuits (Figure 4b).

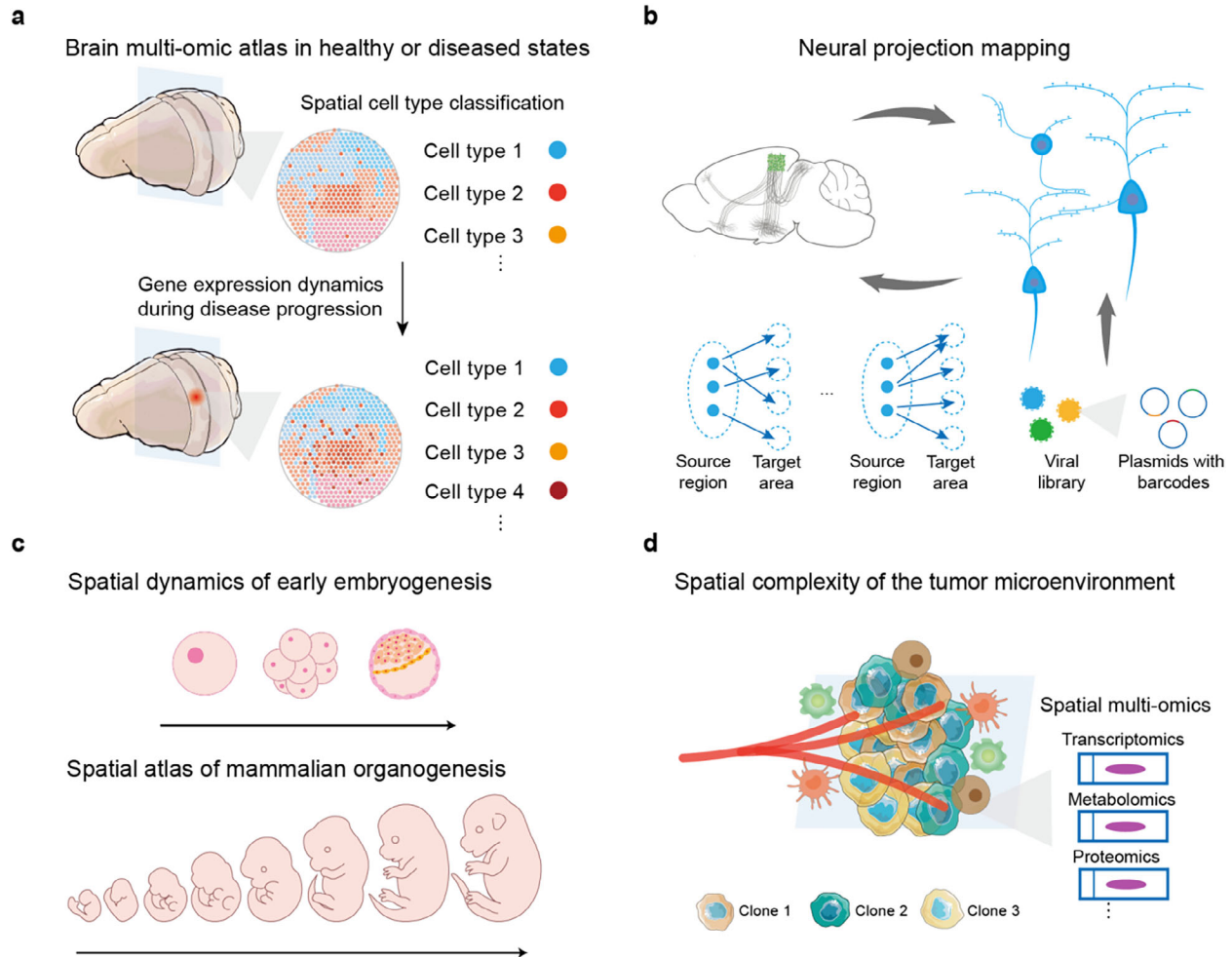


Figure 4. Applications of spatial omics in neurobiology, developmental biology, and cancer biology. a) Brain atlas in regular states or in neurological diseases mapped by spatial omics technologies. b) Spatial neural connecting pattern and neural projection mapping. Reproduced with permission.^[154] Copyright 2019, Elsevier. c) Spatial atlas of early embryogenesis and organogenesis. d) Spatial tumor heterogeneity and complexity of tumor microenvironment resolved by spatial multi-omics.

scRNA-seq technologies have profiled brain cell types at the single-cell transcriptomic and epigenomic levels. Furthermore, scRNA-seq can be combined with morphoelectric measurements, such as Patch-seq, to achieve multimodal integrated cell type classification, encompassing anatomical and electrophysiological properties along with gene expression patterns. However, scRNA-seq requires the dissociation of cells from their brain tissues, resulting in the loss of spatial information about circuit and neighbor interactions. Here, we demonstrate that spatially resolved transcriptomics, such as MERFISH and STARmap, not only provide a census of cell types but also offer opportunities to characterize cellular or subcellular molecular details during behavioral states or diseases, which help us gain a systematic insight into functional brain circuits.

3.1.1. Spatial Atlas of Brain Cell Type Classifications

Advances in ISH methods have enabled the mapping of gene expression in tissue with very high resolution for selected genes. A

comprehensive ISH mapping of the adult mouse brain is compiled in the gene expression atlas generated by the Allen Institute for Brain Science, which details the expression of approximately 20000 genes in coronal and sagittal sections of the entire adult mouse brain, albeit lacking scalable potential and high spatial resolution.^[127] The ST method offers an efficient approach to quantitatively map gene expression in tissue, generating a systematic classification of the adult mouse brain based on the unbiased identification of spatially defining features through whole-brain spatial transcriptomics and coordinate framework of the mouse brain (CCFv3) annotation.^[128]

In recent years, several large-scale projects, particularly the BRAIN Initiative Cell Census Network (BICCN), have significantly enhanced the quality of brain cell-type mapping. In 2023, several studies described comprehensive, brain-wide cell-type atlases with distinct spatial transcriptomics such as MERFISH,^[129,130] Slide-seq,^[131] and STARmap PLUS.^[132] Among image-based spatial technologies, MERFISH is used for spatially profiling cell types in the entire brain or specific subregions at high spatial resolution. BICCN integrates

scRNA-seq data with MERFISH to generate four hierarchical levels of classification—34 classes, 338 subclasses, 1201 super-types, and 5322 clusters—which are subsequently grouped into seven neighborhoods for more in-depth molecular and anatomical analysis.^[130] Two MERFISH-based studies have described the neuronal cell, immature neuronal cell and non-neuronal cell atlas, along with neurotransmitter and neuropeptide expression patterns. For instance, the Subpallium-GABA neighborhood was divided into seven classes, likely reflecting their distinct developmental origins and elucidating the relationship of GABAergic types between hypothalamus and thalamus. In non-neuronal cells, immature neurons in rostral migratory stream (RMS) and subventricular zone (SVZ) share gene expression pattern of *Draxin*, *Prox1*, and *Dcx*, yet exhibit distinct lineage-specific gene patterns in dentate gyrus (DG) and olfactory bulb (OB) trajectories. Moreover, the classification methodology has been refined through the use of spatial modules, spatial gradients, transcription factor hierarchies, and cell-type-specific cell–cell interactions, such as IMN-astrocyte interactions in the OB.^[129,130]

In other comprehensive atlas studies, Langlieb et al. combined snRNA-seq with Slide-seq to highlight neurotransmission and activity-dependent gene enrichment patterns across various cell types and regions.^[131] For instance, activity-regulated genes (ARGs) cluster 6 specific for telencephalic inhibitory neurons includes several genes previously reported as activity-regulated in cortical interneurons, in which many genes are also implicated in dendritic spine development and re-modelling. Shi et al. profile 1022 genes in 3D at a voxel size of $194 \times 194 \times 345 \text{ nm}^3$, mapping 1.09 million high-quality cells across the adult mouse central nervous system using STARmap PLUS, which offers high spatial resolution (200–300 nm).^[132] In this study, the spatial niche gene expression vector of each cell was defined by concatenating its own single-cell gene expression vector with those of its *k*-nearest neighbors (kNNs) in physical space to better integrate spatial information. Consequently, certain molecular tissue regions exhibit spatial gene expression similarities across multiple anatomically defined regions. For example, indusium griseum (IG) and fasciola cinereum (FC) in hippocampal region exhibit high resemblance with CA2 and share cytoarchitecture similarities with, but do not belong to DG. Additionally, the tropism of AAV-PHP.eB across molecular tissue regions and molecular cell types has been assessed through the addition of AAV circular RNA barcodes.

Beyond the comprehensive landscape of the brain, numerous studies focus on specific regions within the brain. Chen et al. utilized BARseq to focus on the whole cortex spatial gene expression pattern, reflecting their modular organization and “wire-by-similarity” relationship.^[133] Di Bella et al. adopted Slide-seqV2 to collect spatial transcriptomes from coronal brain sections at E12.5, E13.5, E15.5, and P1 and used Tangram mapping with corresponding scRNA-seq data to correlate cerebral cortex cell types with spatial distributions.^[134] There is also a comparative study of conservation and divergence of cortical cell organization between mice and humans using MERFISH and expansion microscopy, in which differential interactions between neuronal and non-neuronal cells are more emphasized.^[135]

Using MERFISH, BICCN and others have also specifically characterized spatial cell-type profiles in the mouse primary motor cortex (MOp),^[136–138] hypothalamic nuclei,^[139] and nucleus

accumbens.^[140] In MOp, 258 genes are selected to profile 39 excitatory neuronal clusters, 42 inhibitory neuronal clusters, and 14 non-neuronal clusters.^[136,137] These two studies also observed continuous changes in the gene expression and cortical depth of IT neurons, reflecting a molecular and spatial gradient of cells across the entire cortical depth. In addition to revealing transcriptomic cell-type specificity in the MOp, Boeshaghi et al. extended spatial isoform diversity for cell-type clustering using the combined 10xv3, SMART-seq, and MERFISH data.^[138] Transcriptional regulation like transcription start sites (TSSs) shift and post-transcriptional programs like differential splicing are both examined in this study. In dorsolateral prefrontal cortex (DLPFC), Maynard et al. used the 10x Genomics Visium platform to identify several genes previously underappreciated as laminar markers in human DLPFC, including *AQP4* (L1), *HPCAL1* (L2), *FREM3* (L3), *TRABD2A* (L5), and *KRT17* (L6).^[141]

In hypothalamic preoptic region, 155 genes including known markers for major cell classes or relevant to neuronal functions of the hypothalamus and neuronal cluster markers in scRNA-seq were selected for MERFISH imaging and identified ≈ 40 inhibitory and ~ 30 excitatory neuronal clusters.^[139] Although hypothalamic nuclei lack the laminar features of cortex, spatial technologies can still examine the organization of distinct cell populations that can support defined modes of function within individual hypothalamic nuclei, such as analyzing the relationship between spatial proximity of aromatase- and *Esr1*-expressing cells in paracrine estrogen signaling. In nucleus accumbens, Chen et al. found that different medium spiny neuron (MSN) subtypes exhibit distinct spatial patterns in individual sections by plotting MSN subtypes identified by MERFISH in serial striatal sections.^[140] As for spatial expression patterns in other nuclei structure, Keschull et al. characterized the cerebellar nuclei in mice, chickens, and humans using snRNA-seq and STARmap, identifying a conserved cell-type set that forms an archetypal cerebellar nucleus, representing a fundamental unit of cerebellar nuclei organization and evolution.^[142] Particularly, the mouse OB's spatial expression pattern was first measured by the ST method in 2016, and this data has since been referenced by HDST,^[14] Pixel-seq,^[22] Slide-seqV2,^[16] Stereo-seq^[20] and seqFISH+.^[44] Regarding the spatial distribution of specific cell types, MERFISH analysis on P14 S1 cortex has defined the spatial distribution of microglia states in relation to projection neuron (PN) subtypes.^[143]

In addition to analyzing molecular cytoarchitecture of brain cell atlas at transcriptomic level, spatial epigenomics also aids in understanding nuclear features of brain cells, such as DNA methylome, 3D genome, and chromatin accessibility. Takei et al. use DNA seqFISH+ to image 2460 loci at approximately 1-Mb resolution across the genome and an additional 1200 loci for at least a 1.5-Mb region on each chromosome at 25-kb resolution, which are co-imaged with six histone modifications or variants (H3K4me2, H3K27me2, H3K27me3, H3K9me3, H4K20me3, and mH2A1) by sequential IF.^[144] In this study, a distinctive pattern of proximal points associated with nuclear bodies and chromatin marks for each chromosome forms a scaffold on the exterior of the nuclear bodies in single cells. This arrangement leads to distinct chromosomal positioning and interchromosomal relationships in the nucleus of each cell type, contributing to an epigenomic-level brain atlas. Another study integrated

enhanced single-nucleus methylation sequencing (snmC-seq3) and chromatin conformation capture (3C) sequencing (snm3C-seq) with MERFISH.^[145] The spatial location imputation with single-cell data defines many cell subclasses to complete anatomical structures smaller than our dissection regions, attributed to the strong association between cell location and DNA methylation of crucial genes and regulatory elements. For instance, *Rasgrf2* exhibits differential expression and methylation across cortical layers and differentially methylation regions (DMRs) near *Rasgrf2* are highly correlated. Chromatin conformation data support physical proximity when both the DMR and *Rasgrf2* are active, demonstrating a simple spatial pattern in DNA methylation that aligns with the spatial transcriptome.

3.1.2. Neural Circuits, Multimodal Correspondence, and Behaviors

One of the most distinctive and complex features of the neural system is the long-range projection, which requires building spatial connectivity maps across the different regions or whole brain (Figure 4b). Besides collaborating with electrophysiological technologies,^[146] circuit-level analyses of the mouse brain depend on genetically delivered molecular tools, including anterograde brain mapping using fluorescent or enzymatic labels,^[147] Cre recombinase,^[148] retrograde,^[149] or trans-synaptic viruses^[150] and newly developed RNA editing-based technologies sensing endogenous mRNA transcripts.^[151] However, these approaches can analyze only a few defined subpopulations, potentially missing complex junctions across large regions. Moreover, single-neuron tracing methods are limited by the number of multiplex labeling colors.^[151,152] Therefore, truly high-throughput and high-resolution projection-mapping methods that incorporate spatial information are essential.

There are a series of studies to label neurons by combining injecting a viral library encoding various RNA barcodes with spatial transcriptomics such as MAPseq,^[153] BARseq,^[154] and BARseq2.^[155] In previous work, MAPseq performed reverse transcription on barcode mRNA extracted from dissected target regions, utilizing 12 nt UMI and 6 nt slice specific identifier (SSI) tag to analyze locus coeruleus (LC) projection pattern. This single-neuron resolution analysis revealed that individual LC neurons exhibit idiosyncratic projection patterns with preferred cortical targets, reconciling a controversy about the specificity of LC projection patterns.^[153] A further development, BARseq, uses BaristaSeq and in situ sequencing by synthesis to enhance both the spatial resolution and throughput. Compared to MAPseq, BAR-seq allows for more precise organization of projections across neuronal subtypes, such as a projection pattern (ITi-Ctx) almost entirely restricted to two transcriptionally defined IT subtypes.^[154] This technology also describes the neuron connectivity throughout the entire cortex.^[133] The advanced version BARseq2 features a larger gene detection range and enhanced sensitivity by using multiple probes for each target mRNA and a non-gap-filled padlock probe-based approach to amplify target transcripts, identifying modest associations between 65 cadherins' expression and projections in IT neurons.^[155] Moreover, MAPseq and BARseq can be integrated to identify multiple bulb-to-piriform cortex projection gradients, demonstrating that OB-to-piriform cortex connectivity contains both distributed and spatially organized components.^[156]

Other integration of retrograde tracing methods with spatial transcriptomics such as MERFISH (Retro-MERFISH) has identified projection targets of various neuron types in the MOp.^[137] Long-range axon projection patterns of individual glutamatergic excitatory neurons exhibit complex and diverse relationships with transcriptomic and epigenetic types. Besides retrograde tracing strategy, "functional neuromics" involves using two-photon microscopy to record from large populations of neurons in mouse V1, followed by applying IST to the imaged tissue to localize mRNAs for 72 selected genes.^[157] Using MERFISH solely, projection neurons (PNs) are specifically measured and the presence of PN-responsive microglia is verified, revealing finely controlled interactions between multiple cell types with the local cortical circuits.^[143]

Spatial omics also play an important role in understanding the neural circuits behind certain behaviors, including long-term memory,^[158,159] fever and appetite during sickness,^[160] odor processing,^[161] and discrete social behaviors such as parenting, aggression, or mating.^[139] Using a combination of scRNA-seq and Slide-seqV2, Wang et al. generated a map of most glomerular positions in the mouse OB and discovered that each type of olfactory sensory neuron (OSN) expresses a unique transcriptional program to sufficiently predict the OSN axon projection to form a glomerulus.^[161] Regarding memory consolidation, CA1 subregion-specific expression of a transcription factor subfamily and neuron-astrocyte synergy were both confirmed in encoding long-term memory, identified through spatial transcriptomics.^[158,159] Furthermore, an integrated analysis with CaRNA (calcium and RNA multiplexed activity) imaging platform and multiplex RNA FISH validates the molecularly defined spatial cell types, reducing the dimensionality of the hypothalamic paraventricular nucleus (PVH) neuronal ensemble.^[162] This approach enhances our understanding of behavioral state coding and offers a more comprehensive view of functional neuron dynamics.

3.1.3. Spatial Patterns in Pathology and Diseases of the Neural System

In various neurodegenerative diseases, distinct neuronal populations are selectively vulnerable to pathogenic processes, which has also been used to describe the selective accumulation of pathological protein aggregates in certain neurons, or the selective dysfunction of particular neuronal types.^[163] Spatial transcriptomic approaches enable the transition from inaccurate anatomical descriptions of selectively vulnerable neurons to more detailed characterizations with high spatial resolution. In some sclerosis diseases like amyotrophic lateral sclerosis (ALS)^[164] and progressive multiple sclerosis (MS),^[165] spatial transcriptomics and proteomics are used to analyze tissue slides from different stages to capture spatiotemporal dynamics of molecular pathology.

In Alzheimer's Disease (AD), a comprehensive spatial transcriptomic analysis in mouse AD model uses ST and orthogonal ISS to describe adjacent cell types in a 100- μ m diameter around amyloid plaques.^[166] This study finds that plaque-induced genes (PIGs) representing intercellular cross-talk between astrocytes and microglia concomitantly alter the classical complement system and endosomal/lysosomal pathways, and dynamic

oligodendrocyte genes (OLIGs) response represents myelin-related genes of oligodendrocytes and is modulated by gradual amyloid accumulation. Another study also checks the PIGs changes in cells with various distances to plaque and particularly focuses on Trem2, one of the genes upregulated specifically on plaques in NLF and NLGF mice and specially mentioned in ALS studies.^[164,167] A study with STARmap PLUS draws a comprehensive transcriptomic atlas of AD at a voxel size of $95 \times 95 \times 350$ nm during the development of amyloid plaque and tau pathology in TauPS2APP triple transgenic mice.^[123] It further proposes a glial core-shell structure around $A\beta$ plaques where the disease-associated microglia (DAM) emerge early as the core at an early stage, and the shell is a gliogenesis zone enriched for disease-associated astrocyte-like (DAA-like) cells, OPC and oligodendrocytes that develop at a later stage. Other spatial omics such as proteomics based on Nanostring GeoMx DSP are also used to measure p-tau-positive neurofibrillary tangles (NFTs) in AD or primary age-related tauopathy (PART).^[168]

In neuropsychiatric disorders, pathologies and gene expression differences are often confined to specific cortical layers. Maynard et al. generated spatial gene expression maps in the six-layered DLPFC based on 10x Genomics Visium platform to better understand the regulation of synaptically localized transcripts, which determines the maintenance of synapses in key circuits and further the impairment pattern in schizophrenia disorder (SCZD) or autism spectrum disorder (ASD).^[142] Another study on DLPFC using the Visium platform found that compositional changes in a subset of principal and GABAergic neurons have a more pronounced effect on the upper cortical layers compared to the lower layers.^[169] Additionally, the granule cell layer of the dentate gyrus (DG-GCL) in the human hippocampus has been profiled by LCM-seq, revealing that deficits in activity in these granule neurons and downstream target CA3 in pattern completion are associated with bipolar disorder and schizophrenia.^[170] Furthermore, in a molecular atlas study, spiny projection neurons (SPN) clusters with the strongest enrichment for schizophrenia heritability express markers of an eSPN identity, such as Casz1, Htr7, and Col11a1.^[131] These neurons are found located in both the dorsal and ventral striatum as well as other striatal and pallidal structures, suggesting the potential importance of corticostriatal circuitry in the pathogenesis of schizophrenia. Besides, spatial omics can be used in other nervous system diseases and mentioned more clearly in previous reviews.^[171–173]

3.2. Spatial Omics in Developmental Biology

In developmental biology, the necessity for spatial transcriptomics arises from the need to understand the intricate spatial and temporal dynamics of gene expression throughout development. Spatial technologies enable researchers to observe not only the expression of genes at the single-cell level but also their spatial distribution across various developmental stages. Capturing these changes in specific regions and times within developing tissues highlights the complex interactions including tissue differentiation, organ development, and cell fate determination. Spatial transcriptomics offers a comprehensive view of the cellular composition and architectural complexities of developing tissues, which is essential for decoding the multifaceted nature of biological development.

3.2.1. Spatiotemporal Atlas of Mammalian Organogenesis

Mammalian organogenesis is a complex process where cells from the three germ layers transform into an embryo with major organs within just a few days (Figure 4c). At the early-somite stages in model organisms like mice, the embryo transitions from gastrulation to early organogenesis, along with brain compartmentalization and neural tube folding (embryonic days (E) 8.0–9.5 in mice).^[174] In the ensuing days (E9.5–E13.5), the embryo rapidly expands to ten million cells and establishes the major organ system, a critical stage for organoid studies and tissue engineering.^[175,176] In studies of spatiotemporal dynamics during organogenesis, spatial omics can provide molecular evidence of developmental trajectories and spatial distribution with similar origins.

DBiT-seq has been employed to profile the whole embryo, embryonic brain, and early eye development of the E10 mouse embryo at 50 μ m, 25 μ m, and 10 μ m resolution respectively.^[24] Spatially resolved, embryo-scale transcriptomic atlas constructions have also been achieved using other methods such as sci-Space,^[19] Stereo-seq,^[20] seqFISH,^[177] Slide-seq^[178] and Visium.^[179,180] Three-dimensional embryo reconstruction approaches, particularly with the help of bioinformatic tools and stacked sections, have become increasingly prevalent.^[178,179] Analyzing samples of E9.5–E16.5 mouse embryos by Stereo-seq, Chen et al. revealed spatial cell-type heterogeneity and mapped the long-time-range dynamics of mouse organogenesis at cellular resolution.^[20]

Transitioning from the whole embryo cell clustering to more specific organs, the developing brain is frequently discussed and spatially profiled due to its complex diversifications and indistinct boundaries. For instance, the dynamics of progenitor cell differentiation in the dorsal midbrain at E12.5, E14.5, and E16.5 are investigated using Stereo-seq.^[20] At the early organogenesis stages, such as E8.5, spatial patterns of gene expression at the midbrain–hindbrain boundary (MHB) are verified using seqFISH.^[177] As for E8.5–E9.5, Kumar et al. used Slide-seq to find that several genes including epigenetic and metabolic regulators exhibit regionalized expressions along antero-posterior (AP) and DV axes.^[178] A more comprehensive atlas combining scRNA-seq and in situ sequencing profiles the functional elements of the brain and its enclosing membranes, including the early neuroepithelium, region-specific secondary organizers, as well as neurogenic and gliogenic progenitors.^[181]

Beyond the mouse brain, there are also studies focusing on other specific organs, particularly smaller regions. At the E10 stage, a nearly late optic vesicle stage of eye development, genes such as Pax6, Pme1, Six6, and Trpm1 are identified with distinct but spatially correlated expression patterns.^[24] Additionally, at the E12.5 stage, Aldh1a3 and Col9a1 are identified as spatially enriched genetic drivers of ocular development disorders using Slide-seqV2.^[16] Osteogenesis and limb development are also spatially mapped using Visium and TATTOO-seq, respectively.^[180,182]

Epigenetic reprogramming usually plays a critical spatiotemporal regulatory role throughout developmental periods, involving changes in the 3D genome, chromatin accessibility, and histone modifications.^[10,183] For instance, using MINA, a promoter-enhancer interaction pattern in the cis-regulatory region of Scd2

enriched in E14.5 mouse embryonic liver was identified.^[84] Co-mapping of spatial ATAC and RNA using MISAR-seq predicts the signature TFs for each developing brain cell cluster based on the differential peaks, identifies key regulators, and decodes the gene regulatory network especially during corticogenesis.^[118] Based on DBiT-seq, spatial-ATAC-seq, spatial-CUT&Tag and their combinations with spatial RNA-seq jointly provide a spatially epigenetic landscape of the mouse embryo, particularly highlighting brain development and neuronal differentiation.^[7,96,118] Similarly, Epigenomic MERFISH reveals putative active enhancers and their refined spatial patterns by targeting genomic loci with the H3K27ac modification in the E13.5 mouse embryonic brain.^[10]

While the mouse serves as a fundamental model organism in embryonic studies, research on human embryos remains indispensable for translational considerations. Recently, the construction of the spatial transcriptomic atlas has expanded to include various developing human organs such as the heart,^[184,185] pancreas,^[186] limb,^[187] spinal cord,^[188,189] and brain.^[190] Additionally, other model species such as zebrafish, drosophila, and axolotl have also been profiled for embryogenesis studies using Tomo-seq^[27,191] and Stereo-seq.^[192–194]

3.2.2. Spatial Layer Expression Distribution in Early Embryo Stages

Post-implantation mouse development represents a complex stage of early embryogenesis, particularly during gastrulation. In mammalian gastrulation, the primary germ layers are formed, and multipotent embryonic cells are allocated to the progenitors of various tissue lineages within the germ layers. The morphogenesis of the germ layers during this stage involves complex mechanisms that regulate cell movement and differentiation, driving lineage specification and tissue modeling in the embryo.^[195,196] Peng et al. utilized Geo-seq to explore mouse embryogenesis from the late mid-streak stage (E7) through stages from pre-gastrulation to late gastrulation (E5.5–E7.5) successively.^[197,198] To establish lineage trajectory, RNA-seq data from E2.5, E3.5, and E4.5 were further co-analyzed with Geo-seq data using single-cell regulatory network inference and clustering (SCENIC) pipeline.^[198] For cell niches and cell-cell adjacency analysis, ClusterMap provides multi-scale clustering in the mouse placenta based on density peak clustering (DPC).^[199] At later stages like E8.5, integrative seqFISH analysis can effectively spatially define five subpopulations of mixed mesenchymal mesoderm, which is more considered as a cell state rather than a cell type and challenging to distinguish subtle subtypes in scRNA-seq.^[177]

In addition to mouse gastrulation, primate gastrulation at-lases, including those for monkey and human, have also been established.^[200,201] Particularly in studies of the intact Carnegie stage (CS) 8 human embryo, spatial patterns of cell types across different germ layers and key signaling pathways have been revealed through a 3D reconstruction model.^[201] In the stages preceding human gastrulation, the mechanisms by which extravillous trophoblasts (EVTs) coordinate with the maternal decidua to promote a tissue microenvironment conducive to spiral artery remodeling (SAR) remain a subject of debate.^[202,203] Two recent studies have investigated trophoblast cell trajectories and interactions between immune cells and stromal cells respectively at the

early maternal-fetal interface, using spatial transcriptomics and proteomics based on MIBI-TOF and GeoMx DSP.^[204,205] During embryogenesis stages such as the PN4 zygote, late two-cell, and early four-cell stages, the remodeling of chromatin organizations primes the organism for zygotic genome activation (ZGA) and lineage-specific cell fates are more concerned, and can be observed using IGS.^[88]

3.2.3. Spatially Resolved Organoids and Aging Organs

Organoids derived from stem cells, capable of differentiating and self-organizing in 3D space, have emerged as an important tool for studying human development and modeling the complex characteristics of human diseases in vitro.^[206] However, quantitative measurements across different spatial scales and molecular modalities remain lacking. Using Slide-seqV2, the spatial organization of cell types in cortical organoids at 1, 2, and 3 months displays high levels of developmental fidelity, reproducibility, and reliable molecular programs, irrespective of metabolic state.^[207] Spatial proteomics of 3D human pluripotent stem cell-derived cyst (hPSC-cyst) structures have also been analyzed using APEX2-based proximity biotinylation, followed by mass spectrometry.^[208] Another spatial proteomics map of human retinal organoids and adult retina, based on iterative indirect immunofluorescence imaging (4i), are generated covering organoid development timescale (6, 12, 18, 24, and 39 weeks).^[209] In this study, retinal layer formation and neurogenesis have been reconstructed with scATAC-seq and scRNA-seq. Additionally, transcriptional factor perturbation experiments using CROP-seq^[210] have explored the effects of several genes on the spatiotemporal dynamics in retinal organoids, especially OTX2. Another functional omics combining optogenetic perturbation and Visium locally activates Sonic Hedgehog (SHH) signaling in an organoid model for human neurodevelopment, proving sufficient to generate stereotypically patterned organoids.^[211]

Beyond the study of life's beginnings, such as fertilization and embryogenesis, aging represents another important theme in developmental biology. Cellular senescence, as a trigger of aging and age-related disease, has been increasingly characterized using omics tools. However, two main challenges persist in this field of research: senescent cells are relatively rare and lack a single, definitive marker.^[212,213] Owing to the communication and induction of senescent cells in neighboring cells, spatial omics can pave the way to study the complex and often elusive aging microenvironment.^[214] For instance, a multimodal analysis of age-related changes in the mouse liver microenvironment integrates scATAC-seq, scRNA-seq with Visium and metabolomics to identify chromatin and metabolic remodeling aging factors, particularly lipid and mitochondrial disorder.^[215] Moreover, co-profiling with MERFISH and snRNA-seq in aging mouse brains has revealed pronounced aging changes in non-neuronal cells, along with distinct activation mechanisms and spatial distributions in different non-neuronal cell types such as astrocytes and microglia.^[216]

3.3. Spatial Omics in Cancer Biology

A tumor forms when a cell in a local tissue loses normal growth regulation at the genetic level due to various carcinogenic

factors acting on the body, resulting in its clonal abnormal proliferation. Tumors are not merely a collection of malignant cells; instead, they develop distinct structures that harbor potential mechanisms for carcinogenesis.^[217] Deciphering techniques in cell biology, such as bulk RNA-seq and single-cell sequencing, have provided deep insights into cellular composition and gene expression within tissues, significantly advancing tumor research. However, bulk RNA-seq analyzes tissues in a homogenized state, yielding the average expression levels of tissue cells and obscuring the gene expression profiles of individual cells. On the other hand, single-cell sequencing isolates cells from tissues to create single-cell suspensions, revealing expression profiles of individual genes. This approach is revolutionary for uncovering novel biomarkers and molecular regulators associated with tumor growth, metastasis, and drug resistance. Yet, it inevitably overlooks the spatial context of cells within the original tissue.^[218] Gene expression is both temporally and spatially specific, and the structural and functional properties of tissues depend on the interplay between gene expression and cellular spatial location. Spatial omics techniques can elucidate the spatial distribution of different cell types and their interactions within tumor tissues, contributing to our understanding of cellular evolution and differentiation processes in tumors. This approach unveils the heterogeneity within tumors, paving the way for a comprehensive understanding of the tumor microenvironment and the analysis of potential biological targets (Figure 4d).^[219]

3.3.1. Reveal the Complexity of Tumor Heterogeneity

A central issue in tumor research is the heterogeneity of tumors, which manifests diverse types and states of spatial heterogeneity. Spatial analysis in tumor research provides critical insights into morphology, cellular composition, proximity, and structure.^[220,221] Understanding the shape and size of cells within a tumor is crucial for distinguishing between different cell types.^[222] The composition of cell types within tumors, along with the physical distances between cells and the overall cellular architecture, facilitates comprehension of cell-cell interactions and the distribution of various cell types within tumors.^[57] Analyzing the spatial distribution of different cell types can illuminate the tumor microenvironment and potential therapeutic targets. In recent years, numerous spatial omics techniques have been invented and implemented in diverse areas of cancer research.^[223]

For instance, researchers employ LCM technology to precisely isolate cells from specific regions within tumor tissues for gene expression analysis. Coupled with Smart-3SEQ, this method has compared micro-niches of nasopharyngeal carcinoma epithelial cells with normal cells, revealing vulnerabilities in FGF and non-canonical NF- κ B signaling pathways in tumor samples.^[224] Significant progress has also been achieved with spatially resolved laser-activated cell sorting technology. It employs image-based data for cell classification while preserving spatial information within tissue. Using breast cancer tissue sections, researchers can study the distribution and interactions of diverse cell populations within tumors, gaining deep insights into tumor microenvironments, cellular compositions, and the subclonal and evolutionary relationships between different subpopulations.^[225,226] Additionally, spatial transcriptomics technologies like Visium

and ISS have become pivotal tools in tumor research. Visium technology facilitates high-throughput gene expression analysis on tissue sections, unveiling tumor heterogeneity and revealing new cell states and subgroups.^[227] ISS, on the other hand, examines the spatial distribution of cells within tumor tissues, offering insights into tumor cell heterogeneity and tissue structure.^[228] On the clinical front, comparative analyses of gene expression differences among low-Gleason grade, high-Gleason grade, benign samples, and mesenchymal samples from individual tissue blocks in prostate cancer have helped identify mesenchymal cells that potentially induce metastatic progression.^[228] The dissection of additional genetic heterogeneity of cutaneous malignant melanomas within a spatial context has identified factors regulating tumor progression and clinical outcomes.^[229] Moreover, an increasing number of studies highlight the impact of the spatial composition of tumor subtypes on clinical outcomes,^[230–232] underscoring the importance of identifying tumor heterogeneity in diagnosis, treatment, prognosis, and molecular biomarker analysis.

3.3.2. Understand the Tumor Microenvironment

Describing the spatial context of cells and tissues is a fundamental biological question in cancer research.^[53] The spatial cellular environment provides crucial biological network information about how cells interact with their surroundings.^[233] Tumor cells interact with the nearby microenvironment, shaping the tumor immune microenvironment composed of macrophages, B cells, T cells, dendritic cells, and other immune cells, indicating the reasons behind immune reactions occurring within the tumor structure.^[234–236] From a spatial perspective, the tumor microenvironment (TME) exhibits diverse organizational and hierarchical structures across different tumor types. The TME critically influences the fate and development of cancer cells, regulated by precise intra-tumor transcriptional regulation and intercellular communication.^[237] Therefore, gaining a deeper understanding of the spatial structure of the TME is essential for unraveling tumorigenesis mechanisms and designing crucial new therapeutic strategies.^[238] Spatial analysis and the application of multiplexing techniques in oncology research have provided profound insights into the TME and its pivotal role in cancer development and therapy.

For instance, multiplexed smFISH techniques have been extensively used to characterize the expression of hundreds of genes in immune and cancer cells, concurrently assessing the role of the tumor microenvironment in transitioning to a mesenchymal-like state.^[239] Alissa et al. combine spatial transcriptomics, spatial proteomics, and computational approaches to define glioma cellular states and uncover their organization, providing a conceptual framework for the organization of cellular states in glioma, highlighting hypoxia as a long-range tissue organizer.^[240] Additionally, the spatial localization of 297 tumor-associated genes, coupled with expanding microscopy techniques, has revealed the complex structure and function of the tumor microenvironment.^[50,241] Spatial analysis of tissue architecture has been actively employed to unveil unique tumor structures like tertiary lymphoid structures (TLS), immune cell-rich formations indicative of ongoing anti-tumor immune responses.^[242] GeoMx DSP has highlighted a significant

presence of the checkpoint protein CTLA4 around pancreatic ductal adenocarcinomas, supporting the hypothesis that tumors evade adaptive immune responses induced by gene overexpression.^[243]

By analyzing the spatial distribution of tumor structures, researchers have gained deeper insights into the characterization of the tumor microenvironment.^[244,245] For example, Ji et al. employed single-cell transcriptome sequencing of human squamous skin carcinomas and matched normal skin, along with spatial transcriptome sequencing, to elucidate the cellular composition and structure of these tumors.^[246] They revealed that tumor-specific glial cells located primarily at tumor growth fronts act as hubs of intercellular communication, expressing genes that recruit specific cell populations, defining subpopulations of squamous cell carcinoma and stromal cells, and elucidating the spatial microenvironments and communication networks involved in tumorigenesis. Wu et al. utilized spatial multi-omics to analyze the spatial localization of breast cancer histiocytes, tumor-associated immune cells, and stromal cells, observing that T cells predominantly inhabit lymphocyte-rich regions and regions composed of stromal cells and lymphocytes, with positive correlations between the locations of CD4⁺ T cells, CD8⁺ T cells, and ApoE⁺ macrophages.^[247]

3.3.3. Identify Potential Therapeutic Targets

Drug resistance and cancer treatment strategies are significantly influenced by the spatial structure of tumors. By analyzing patterns of gene expression and protein distribution within different tumor regions, researchers can unveil complex biological features at both tissue and cellular levels, identify key molecules that may impact therapeutic efficacy, predict drug responsiveness, and reveal mechanisms of therapeutic resistance. This provides essential guidance and support for precision medicine treatments, emphasizing the critical importance of spatially discovering new therapeutic biomarkers.^[236,242,248,249]

For instance, invasive-associated subcellular structural proteins have been identified as potential therapeutic biomarkers.^[250] Ravi et al. utilized spatial transcriptomics, spatial metabolomics, and proteomics approaches to identify essential features of glioblastomas.^[251] They established a microenvironment characterized by immune and metabolic stressors and elucidated localized regional tumor-host interdependence. Spatiotemporal analysis of gliomas revealed the potential of COL1A1 gene suppression in tumor progression, offering clues for developing therapeutic targets.^[252] FISH has been widely employed to map precise spatial information of tumor-specific biomarkers in various tissue samples.^[253] Observations of interactions between FAP⁺ fibroblasts and SPP1⁺ macrophages in colorectal cancers suggest potential tissue remodeling mechanisms and intervention targets.^[254] Spatial molecular typing has proposed novel biomarkers like the cilium gene at the tumor boundary interface, providing robust support for studying tumor spatial biology and discovering therapeutic targets.^[255]

Traditional genomics, transcriptomics, proteomics, and similar methods typically provide information only at the level of specific molecules, without demonstrating their distribution within the tissue structure. Spatial multi-omics technologies address

this limitation by allowing researchers to obtain both molecular information and spatial location information, thereby enhancing our understanding of the complexity within living organisms. By uncovering the spatial distribution and interactions of molecules, researchers can gain a more accurate and comprehensive understanding of tumor biology, which in turn guides the exploration of tumor pathogenesis, the analysis of potential therapeutic targets, and the development of new drugs. Generating spatial maps of human cancers across various histological and temporal scales holds the promise of fundamentally improving our understanding of tumorigenesis. Spatial omics technologies may revolutionize the paradigm of medical research and contribute to the design of advanced therapeutic strategies in the near future.

4. Conclusion and Future Perspectives

The rapid development and integration of spatial omics technologies have led to a new era of exploration in the life sciences, offering unprecedented insights into the spatial organization, interaction, and regulation of biomolecules within biological systems. By utilizing high-throughput techniques like spatial transcriptomics, proteomics, translationalomics, genomics, epigenomics, and metabolomics, researchers have gained a comprehensive understanding of cellular heterogeneity, tissue architecture, and dynamic biological processes. Through the elucidation of key biological phenomena such as nervous system development, organogenesis, and tumor microenvironment dynamics, spatial omics technologies hold immense promise for driving forward our understanding of complex diseases and unlocking innovative therapeutic strategies.

However, despite their remarkable potential, challenges such as technical variability, limited spatial resolution, and the complexity of data analysis remain significant hurdles that need to be addressed. Moreover, the high cost and resource-intensive nature of these techniques may limit their widespread adoption and accessibility in research laboratories. Future commercial advancements in spatial omics technologies will likely focus on overcoming these limitations through the refinement of experimental protocols, the development of novel computational algorithms for data analysis, and the integration of multi-omics approaches.

As for the directions of future technological innovations in spatial omics, several key areas are anticipated. First, there will be a development of more techniques to accommodate various tissue sample types. For instance, FFPE samples have already been utilized in spatial omics to map transcriptomes and proteomes.^[65,256] Moreover, since most current spatial omics techniques are limited to thin tissue sections measuring 5–20 μm , there is a need for methods that can accommodate thicker tissues, enabling 3D architectural profiling. There have already been some pioneering explorations in this area.^[257,258]

Second, there is a need to advance the profiling of spatiotemporal gene regulation at finer levels, such as RNA lifespans and subcellular scales. This could enhance our understanding of cellular organization and molecular interactions. Techniques like metabolic labeling and other time-resolved labeling strategies could facilitate the integration of RNA dynamic processes with different transcriptional and translational phases.^[259] Additionally, combining proximity labeling^[260] and photocatalytic labelling^[261] techniques with spatial omics could yield

spatiotemporal information based on the reaction ranges of enzymes or reactants.

Third, integrating spatially resolved molecular patterns with functional omics or other multimodal profiling approaches presents another significant opportunity. For instance, exploring neural circuits would require the combination of spatial gene expression with neuronal projections mapping^[154] or chronic electrophysiological recording,^[146] benefiting from advancements in spatial omics applicable to thick tissues. Besides, high-throughput genomic perturbation can be efficiently achieved by optical pooled CRISPR screens with spatial barcodes, which can then be linked to the downstream gene expression variation.^[262–264]

Furthermore, the application of spatial omics technologies in clinical settings holds great potentials for personalized medicine and precision therapeutics. By providing spatially resolved molecular profiles of diseased tissues, these technologies offer opportunities for early diagnosis, prognosis prediction, and targeted treatment strategies tailored to individual patients. In summary, while spatial omics technologies have already significantly advanced our understanding of biological complexity, their ongoing development and refinement are essential for unlocking deeper insights into the intricacies of living organisms and translating these discoveries into clinical practice.

Acknowledgements

T.H. and J.Z. contributed equally to this work. This study received support from the National Key Research and Development Program of China (2024YFC3405600 and 2024YFF0507400 to H.Z.), the Frontier Innovation Fund of Peking University Chengdu Academy for Advanced Interdisciplinary Biotechnologies, the Center for Life Sciences (CLS), and the College of Future Technology (CFT) of Peking University.

Conflict of Interest

The authors declare no conflict of interest.

Keywords

cancer biology, developmental biology, neurobiology, spatial omics, spatial transcriptomics

Received: July 29, 2024
Revised: March 3, 2025
Published online:

- [1] D. Bressan, G. Battistoni, G. J. Hannon, *Science* **2023**, *381*, eabq4964.
- [2] K. Vandereyken, A. Sifrim, B. Thienpont, T. Voet, *Nat. Rev. Genet.* **2023**, *24*, 494.
- [3] L. Moses, L. Pachter, *Nat. Methods* **2022**, *19*, 534.
- [4] S. Jain, M. T. Eadon, *Nat. Rev. Nephrol.* **2024**, *20*, 659.
- [5] S. M. Lewis, M.-L. Asselin-Labat, Q. Nguyen, J. Berthelet, X. Tan, V. C. Wimmer, D. Merino, K. L. Rogers, S. H. Naik, *Nat. Methods* **2021**, *18*, 997.
- [6] S. Lee, G. Kim, J. Lee, A. C. Lee, S. Kwon, *Mol. Cancer* **2024**, *23*, 26.

- [7] D. Zhang, Y. Deng, P. Kukanja, E. Agirre, M. Bartosovic, M. Dong, C. Ma, S. Ma, G. Su, S. Bao, Y. Liu, Y. Xiao, G. B. Rosoklija, A. J. Dwork, J. J. Mann, K. W. Leong, M. Boldrini, L. Wang, M. Haeussler, B. J. Raphael, Y. Kluger, G. Castelo-Branco, R. Fan, *Nature* **2023**, *616*, 113.
- [8] E. Lundberg, G. H. H. Borner, *Nat. Rev. Mol. Cell Biol.* **2019**, *20*, 285.
- [9] T. Zhao, Z. D. Chiang, J. W. Morriss, L. M. LaFave, E. M. Murray, I. Del Priore, K. Meli, C. A. Lareau, N. M. Nadaf, J. Li, A. S. Earl, E. Z. Macosko, T. Jacks, J. D. Buenrostro, F. Chen, *Nature* **2022**, *601*, 85.
- [10] T. Lu, C. E. Ang, X. Zhuang, *Cell* **2022**, *185*, 4448.
- [11] K. D. G. Saunders, H.-M. Lewis, D. J. Beste, O. Cexus, M. J. Bailey, *Curr. Opin. Chem. Biol.* **2023**, *75*, 102327.
- [12] L. Tian, F. Chen, E. Z. Macosko, *Nat. Biotechnol.* **2023**, *41*, 773.
- [13] P. L. Ståhl, F. Salmén, S. Vickovic, A. Lundmark, J. F. Navarro, J. Magnusson, S. Giacomello, M. Asp, J. O. Westholm, M. Huss, A. Mollbrink, S. Linnarsson, S. Codeluppi, Å. Borg, F. Pontén, P. I. Costea, P. Sahlén, J. Mulder, O. Bergmann, J. Lundeberg, J. Frisén, *Science* **2016**, *353*, 78.
- [14] S. Vickovic, G. Eraslan, F. Salmén, J. Klughammer, L. Stenbeck, D. Schapiro, T. Äijö, R. Bonneau, L. Bergensträhle, J. F. Navarro, J. Gould, G. K. Griffin, Å. Borg, M. Ronaghi, J. Frisén, J. Lundeberg, A. Regev, P. L. Ståhl, *Nat. Methods* **2019**, *16*, 987.
- [15] S. G. Rodrigues, R. R. Stickels, A. Goeva, C. A. Martin, E. Murray, C. R. Vanderburg, J. Welch, L. M. Chen, F. Chen, E. Z. Macosko, *Science* **2019**, *363*, 1463.
- [16] R. R. Stickels, E. Murray, P. Kumar, J. Li, J. L. Marshall, D. J. Di Bella, P. Arlotta, E. Z. Macosko, F. Chen, *Nat. Biotechnol.* **2021**, *39*, 313.
- [17] A. J. C. Russell, J. A. Weir, N. M. Nadaf, M. Shabet, V. Kumar, S. Kambhampati, R. Raichur, G. J. Marrero, S. Liu, K. S. Balderrama, C. R. Vanderburg, V. Shanmugam, L. Tian, J. B. Iorgulescu, C. H. Yoon, C. J. Wu, E. Z. Macosko, F. Chen, *Nature* **2024**, *625*, 101.
- [18] Y. Lee, D. Bogdanoff, Y. Wang, G. C. Hartoularos, J. M. Woo, C. T. Mowery, H. M. Nisonoff, D. S. Lee, Y. Sun, J. Lee, S. Mehdiadeh, J. Cantlon, E. Shifrut, D. N. Ngyuen, T. L. Roth, Y. S. Song, A. Marson, E. D. Chow, C. J. Ye, *Sci. Adv.* **2021**, *7*.
- [19] S. R. Srivatsan, M. C. Regier, E. Barkan, J. M. Franks, J. S. Packer, P. Grosjean, M. Duran, S. Saxton, J. J. Ladd, M. Spielmann, C. Lois, P. D. Lampe, J. Shendure, K. R. Stevens, C. Trapnell, *Science* **2021**, *373*, 111.
- [20] A. Chen, S. Liao, M. Cheng, K. Ma, L. Wu, Y. Lai, X. Qiu, J. Yang, J. Xu, S. Hao, X. Wang, H. Lu, X. Chen, X. Liu, X. Huang, Z. Li, Y. Hong, Y. Jiang, J. Peng, S. Liu, M. Shen, C. Liu, Q. Li, Y. Yuan, X. Wei, H. Zheng, W. Feng, Z. Wang, Y. Liu, Z. Wang, et al., *Cell* **2022**, *185*, 1777.
- [21] C.-S. Cho, J. Xi, Y. Si, S.-R. Park, J.-E. Hsu, M. Kim, G. Jun, H. M. Kang, J. H. Lee, *Cell* **2021**, *184*, 3559.
- [22] X. Fu, L. Sun, R. Dong, J. Y. Chen, R. Silakit, L. F. Condon, Y. Lin, S. Lin, R. D. Palmiter, L. Gu, *Cell* **2022**, *185*, 4621.
- [23] J. Cao, Z. Zheng, D. Sun, X. Chen, R. Cheng, T. Lv, Y. An, J. Zheng, J. Song, L. Wu, C. Yang, *Nat. Biotechnol.* **2024**, *42*, 1735.
- [24] Y. Liu, M. Yang, Y. Deng, G. Su, A. Enniful, C. C. Guo, T. Tebaldi, D. Zhang, D. Kim, Z. Bai, E. Norris, A. Pan, J. Li, Y. Xiao, S. Halene, R. Fan, *Cell* **2020**, *183*, 1665.
- [25] M. R. Emmert-Buck, R. F. Bonner, P. D. Smith, R. F. Chuaqui, Z. Zhuang, S. R. Goldstein, R. A. Weiss, L. A. Liotta, *Science* **1996**, *274*, 998.
- [26] S. Nichterwitz, G. Chen, J. Aguila Benitez, M. Yilmaz, H. Storrall, M. Cao, R. Sandberg, Q. Deng, E. Hedlund, *Nat. Commun.* **2016**, *7*, 12139.
- [27] J. P. Junker, E. S. Noël, V. Guryev, K. A. Peterson, G. Shah, J. Huisken, A. P. McMahon, E. Berezikov, J. Bakkers, A. van Oudenaarden, *Cell* **2014**, *159*, 662.

- [28] J. Chen, S. Suo, P. P. Tam, J.-D. J. Han, G. Peng, N. Jing, *Nat. Protoc.* **2017**, *12*, 566.
- [29] H. H. Schede, C. G. Schneider, J. Stergiadou, L. E. Borm, A. Ranjak, T. M. Yamawaki, F. P. A. David, P. Lönnerberg, M. A. Tosches, S. Codeluppi, G. L. a. Manno, *Nat. Biotechnol.* **2021**, *39*, 968.
- [30] C. Medaglia, A. Giladi, L. Stoler-Barak, M. De Giovanni, T. M. Salame, A. Biram, E. David, H. Li, M. Iannacone, Z. Shulman, I. Amit, *Science* **2017**, *358*, 1622.
- [31] A. S. Genshaft, C. G. K. Ziegler, C. N. Tzouanas, B. E. Mead, A. M. Jaeger, A. W. Navia, R. P. King, M. D. Mana, S. Huang, V. Mitsialis, S. B. Snapper, Ö. H. Yilmaz, T. Jacks, J. F. Van Humbeck, A. K. Shalek, *Nat. Commun.* **2021**, *12*, 4995.
- [32] K. H. Hu, J. P. Eichorst, C. S. McGinnis, D. M. Patterson, E. D. Chow, K. Kersten, S. C. Jameson, Z. J. Gartner, A. A. Rao, M. F. Krummel, *Nat. Methods* **2020**, *17*, 833.
- [33] D. Lovatt, B. K. Ruble, J. Lee, H. Dueck, T. K. Kim, S. Fisher, C. Francis, J. M. Spaethling, J. A. Wolf, M. S. Grady, A. V. Ulyanova, S. B. Yeldell, J. C. Gripenburg, P. T. Buckley, J. Kim, J.-Y. Sul, I. J. Dmochowski, J. Eberwine, *Nat. Methods* **2014**, *11*, 190.
- [34] M. Honda, S. Oki, R. Kimura, A. Harada, K. Maehara, K. Tanaka, C. Meno, Y. Ohkawa, *Nat. Commun.* **2021**, *12*, 4416.
- [35] C. R. Merritt, G. T. Ong, S. E. Church, K. Barker, P. Danaher, G. Geiss, M. Hoang, J. Jung, Y. Liang, J. McKay-Fleisch, K. Nguyen, Z. Norgaard, K. Sorg, I. Sprague, C. Warren, S. Warren, P. J. Webster, Z. Zhou, D. R. Zollinger, D. L. Dunaway, G. B. Mills, J. M. Beechem, *Nat. Biotechnol.* **2020**, *38*, 586.
- [36] J. Y. Kishi, N. Liu, E. R. West, K. Sheng, J. J. Jordanides, M. Serrata, C. L. Cepko, S. K. Saka, P. Yin, *Nat. Methods* **2022**, *19*, 1393.
- [37] J. G. Gall, M. L. Pardue, *Proc. Natl. Acad. Sci. USA* **1969**, *63*, 378.
- [38] R. Ke, M. Mignardi, A. Pacureanu, J. Svedlund, J. Botling, C. Wählby, M. Nilsson, *Nat. Methods* **2013**, *10*, 857.
- [39] H. A. John, M. L. Birnstiel, K. W. Jones, *Nature* **1969**, *223*, 582.
- [40] A. M. Femino, F. S. Fay, K. Fogarty, R. H. Singer, *Science* **1998**, *280*, 585.
- [41] K. H. Chen, A. N. Boettiger, J. R. Moffitt, S. Wang, X. Zhuang, *Science* **2015**, *348*, aaa6090.
- [42] C. Xia, J. Fan, G. Emanuel, J. Hao, X. Zhuang, *Proc. Natl. Acad. Sci. USA* **2019**, *116*, 19490.
- [43] E. Lubeck, A. F. Coskun, T. Zhiyentayev, M. Ahmad, L. Cai, *Nat. Methods* **2014**, *11*, 360.
- [44] C.-H. L. Eng, M. Lawson, Q. Zhu, R. Dries, N. Koulana, Y. Takei, J. Yun, C. Cronin, C. Karp, G.-C. Yuan, L. Cai, *Nature* **2019**, *568*, 235.
- [45] S. Codeluppi, L. E. Borm, A. Zeisel, G. L. a. Manno, J. A. van Lunteren, C. I. Svensson, S. Linnarsson, *Nat. Methods* **2018**, *15*, 932.
- [46] J. H. Lee, E. R. Daugharthy, J. Scheiman, R. Kalhor, J. L. Yang, T. C. Ferrante, R. Terry, S. S. F. Jeanty, C. Li, R. Amamoto, D. T. Peters, B. M. Turczyk, A. H. Marblestone, S. A. Inverso, A. Bernard, P. Mali, X. Rios, J. Aach, G. M. Church, *Science* **2014**, *343*, 1360.
- [47] X. Chen, Y.-C. Sun, G. M. Church, J. H. Lee, A. M. Zador, *Nucleic Acids Res.* **2018**, *46*, e22.
- [48] X. Wang, W. E. Allen, M. A. Wright, E. L. Sylwestrak, N. Samusik, S. Vesuna, K. Evans, C. Liu, C. Ramakrishnan, J. Liu, G. P. Nolan, F.-A. Bava, K. Deisseroth, *Science* **2018**, *361*, eaat5691.
- [49] D. Gyllborg, C. M. Langseth, X. Qian, E. Choi, S. M. Salas, M. M. Hilscher, E. S. Lein, M. Nilsson, *Nucleic Acids Res.* **2020**, *48*, e112.
- [50] S. Alon, D. R. Goodwin, A. Sinha, A. T. Wassie, F. Chen, E. R. Daugharthy, Y. Bando, A. Kajita, A. G. Xue, K. Marrett, R. Prior, Y. Cui, A. C. Payne, C.-C. Yao, H.-J. Suk, R. Wang, C.-C. J. Yu, P. Tillberg, P. Reginato, N. Pak, S. Liu, S. Punthambaker, E. P. R. Iyer, R. E. Kohman, J. A. Miller, E. S. Lein, A. Lako, N. Cullen, S. Rodig, K. Helvie, et al., *Science* **2021**, *371*, eaax2656.
- [51] F. Chen, P. W. Tillberg, E. S. Boyden, *Science* **2015**, *347*, 543.
- [52] L. Li, C. Sun, Y. Sun, Z. Dong, R. Wu, X. Sun, H. Zhang, W. Jiang, Y. Zhou, X. Cen, S. Cai, H. Xia, Y. Zhu, T. Guo, K. D. Piatkevich, *Nat. Commun.* **2022**, *13*, 7242.
- [53] C. Giesen, H. A. O. Wang, D. Schapiro, N. Zivanovic, A. Jacobs, B. Hattendorf, P. J. Schüffler, D. Grolimund, J. M. Buhmann, S. Brandt, Z. Varga, P. J. Wild, D. Günther, B. Bodenmiller, *Nat. Methods* **2014**, *11*, 417.
- [54] E. N. Kim, P. Z. Chen, D. Bressan, M. Tripathi, A. Miremadi, M. di Pietro, L. M. Coussens, G. J. Hannon, R. C. Fitzgerald, L. Zhuang, Y. H. Chang, *Cell Rep Methods* **2023**, *3*, 100595.
- [55] S. Rost, J. Giltneane, J. M. Bordeaux, C. Hitzman, H. Koeppen, S. D. Liu, *Lab. Invest.* **2017**, *97*, 992.
- [56] J. Ptacek, D. Locke, R. Finck, M.-E. Cvjick, Z. Li, J. G. Tarolli, M. Aksoy, Y. Sigal, Y. Zhang, M. Newgren, J. Finn, *Lab. Invest.* **2020**, *100*, 1111.
- [57] J. W. Hickey, E. K. Neumann, A. J. Radtke, J. M. Camarillo, R. T. Beuschel, A. Albanese, E. McDonough, J. Hatler, A. E. Wiblin, J. Fisher, J. Croteau, E. C. Small, A. Sood, R. M. Caprioli, R. M. Angelo, G. P. Nolan, K. Chung, S. M. Hewitt, R. N. Germain, J. M. Spraggins, E. Lundberg, M. P. Snyder, N. L. Kelleher, S. K. Saka, *Nat. Methods* **2022**, *19*, 284.
- [58] A. Kinkhabwala, C. Herbel, J. Pankratz, D. A. Yushchenko, S. Rüberg, P. Praveen, S. Reiß, F. C. Rodriguez, D. Schäfer, J. Kollet, V. Dittmer, M. Martinez-Osuna, L. Minnerup, C. Reinhard, A. Dzionek, T. D. Rockel, S. Borbe, M. Büscher, J. Krieg, M. Nederlof, M. Jungblut, D. Eckardt, O. Hardt, C. Dose, E. Schumann, R.-P. Peters, S. Miltenyi, J. Schmitz, W. Müller, A. Bosio, *Sci. Rep.* **2022**, *12*, 1911.
- [59] W. Schubert, B. Bonnekoh, A. J. Pommer, L. Philipsen, R. Böckelmann, Y. Malykh, H. Gollnick, M. Friedenberger, M. Bode, A. W. M. Dress, *Nat. Biotechnol.* **2006**, *24*, 1270.
- [60] J.-R. Lin, M. Fallahi-Sichani, P. K. Sorger, *Nat. Commun.* **2015**, *6*, 8390.
- [61] T. Tsujikawa, S. Kumar, R. N. Borkar, V. Azimi, G. Thibault, Y. H. Chang, A. Balter, R. Kawashima, G. Choe, D. Sauer, E. El Rassi, D. R. Clayburgh, M. F. Kulesz-Martin, E. R. Lutz, L. Zheng, E. M. Jaffee, P. Leyshock, A. A. Margolin, M. Mori, J. W. Gray, P. W. Flint, L. M. Coussens, *Cell Rep.* **2017**, *19*, 203.
- [62] M. Stoeckius, C. Hafemeister, W. Stephenson, B. Houck-Loomis, P. K. Chattopadhyay, H. Swerdlow, R. Satija, P. Smibert, *Nat. Methods* **2017**, *14*, 865.
- [63] S. Black, D. Phillips, J. W. Hickey, J. Kennedy-Darling, V. G. Venkataramanan, N. Samusik, Y. Goltsev, C. M. Schürch, G. P. Nolan, *Nat. Protoc.* **2021**, *16*, 3802.
- [64] Y. Goltsev, N. Samusik, J. Kennedy-Darling, S. Bhate, M. Hale, G. Vazquez, S. Black, G. P. Nolan, *Cell* **2018**, *174*, 968.
- [65] C. M. Schürch, S. S. Bhate, G. L. Barlow, D. J. Phillips, L. Noti, I. Zlobec, P. Chu, S. Black, J. Demeter, D. R. McIlwain, S. Kinoshita, N. Samusik, Y. Goltsev, G. P. Nolan, *Cell* **2020**, *182*, 1341.
- [66] R. Jungmann, M. S. Avendaño, J. B. Woehrstein, M. Dai, W. M. Shih, P. Yin, *Nat. Methods* **2014**, *11*, 313.
- [67] Y. Wang, J. B. Woehrstein, N. Donoghue, M. Dai, M. S. Avendaño, R. C. J. Schackmann, J. J. Zoeller, S. S. H. Wang, P. W. Tillberg, D. Park, S. W. Lapan, E. S. Boyden, J. S. Brugge, P. S. Kaeser, G. M. Church, S. S. Agasti, R. Jungmann, P. Yin, *Nano Lett.* **2017**, *17*, 6131.
- [68] E. M. Unterauer, S. Shetab Boushehri, K. Jevdokimenko, L. A. Masullo, M. Ganji, S. Sograte-Idrissi, R. Kowalewski, S. Strauss, S. C. M. Reinhardt, A. Perovic, C. Marr, F. Opazo, E. F. Fornasiero, R. Jungmann, *Cell* **2024**, *187*, 1785.
- [69] D. Yarilin, K. Xu, M. Turkecul, N. Fan, Y. Romin, S. Fijisawa, A. Barlas, K. Manova-Todorova, *Sci. Rep.* **2015**, *5*, 9534.
- [70] H. M. T. Choi, J. Y. Chang, L. A. Trinh, J. E. Padilla, S. E. Fraser, N. A. Pierce, *Nat. Biotechnol.* **2010**, *28*, 1208.
- [71] R. Lin, Q. Feng, P. Li, P. Zhou, R. Wang, Z. Liu, Z. Wang, X. Qi, N. Tang, F. Shao, M. Luo, *Nat. Methods* **2018**, *15*, 275.

- [72] X. Liu, D. Mao, Y. Song, L. Zhu, A. N. Isak, C. Lu, G. Deng, F. Chen, F. Sun, Y. Yang, X. Zhu, W. Tan, *Sci. Adv.* **2022**, *8*, eabk0133.
- [73] S. He, R. Bhatt, C. Brown, E. A. Brown, D. L. Buhr, K. Chantranuvatana, P. Danaher, D. Dunaway, R. G. Garrison, G. Geiss, M. T. Gregory, M. L. Hoang, R. Khafizov, E. E. Killingbeck, D. Kim, T. K. Kim, Y. Kim, A. Klock, M. Korukonda, A. Kutchma, Z. R. Lewis, Y. Liang, J. S. Nelson, G. T. Ong, E. P. Perillo, J. C. Phan, T. Phan-Everson, E. Piazza, T. Rane, Z. Reitz, et al., *Nat. Biotechnol.* **2022**, *40*, 1794.
- [74] S. K. Saka, Y. Wang, J. Y. Kishi, A. Zhu, Y. Zeng, W. Xie, K. Kirli, C. Yapp, M. Cicconet, B. J. Beliveau, S. W. Lapan, S. Yin, M. Lin, E. S. Boyden, P. S. Kaeser, G. Pihan, G. M. Church, P. Yin, *Nat. Biotechnol.* **2019**, *37*, 1080.
- [75] F. Karlsson, T. Kallas, D. Thiagarajan, M. Karlsson, M. Schweitzer, J. F. Navarro, L. Leijonacker, S. Geny, E. Pettersson, J. Rhomborg-Kauert, L. Larsson, H. van Ooijen, S. Petkov, M. González-Graniillo, J. Bunz, J. Dahlberg, M. Simonetti, P. Sathe, P. Brodin, A. M. Barrio, S. Fredriksson, *Nat. Methods* **2024**, *21*, 1044.
- [76] M. VanInsberghe, J. van den Berg, A. Andersson-Rolf, H. Clevers, A. van Oudenaarden, *Nature* **2021**, *597*, 561.
- [77] H. Zeng, J. Huang, J. Ren, C. K. Wang, Z. Tang, H. Zhou, Y. Zhou, H. Shi, A. Aditham, X. Sui, H. Chen, J. A. Lo, X. Wang, *Science* **2023**, *380*, eadd3067.
- [78] B. A. M. Bouwman, N. Crosetto, M. Bienko, *Trends Genet.* **2022**, *38*, 1062.
- [79] G. Nir, I. Farabella, C. P. Estrada, C. G. Ebeling, B. J. Beliveau, H. M. Sasaki, S. D. Lee, S. C. Nguyen, R. B. McCole, S. Chatteraj, J. Erceg, J. AlHaj Abed, N. M. C. Martins, H. Q. Nguyen, M. A. Hannan, S. Russell, N. C. Durand, S. S. P. Rao, J. Y. Kishi, P. Soler-Vila, M. Di Pierro, J. N. Onuchic, S. P. Callahan, J. M. Schreiner, J. A. Stuckey, P. Yin, E. L. Aiden, M. A. Marti-Renom, C.-T. Wu, *PLoS Genet.* **2018**, *14*, 1007872.
- [80] S. Wang, J.-H. Su, B. J. Beliveau, B. Bintu, J. R. Moffitt, C.-T. Wu, X. Zhuang, *Science* **2016**, *353*, 598.
- [81] B. Bintu, L. J. Mateo, J.-H. Su, N. A. Sinnott-Armstrong, M. Parker, S. Kinrot, K. Yamaya, A. N. Boettiger, X. Zhuang, *Science* **2018**, *362*, eaau1783.
- [82] A. M. Cardozo Gizzi, D. I. Cattoni, J.-B. Fiche, S. M. Espinola, J. Gurgo, O. Messina, C. Houbbron, Y. Ogyama, G. L. Papadopoulos, G. Cavalli, M. Lagha, M. Nollmann, *Mol. Cell* **2019**, *74*, 212.
- [83] L. J. Mateo, S. E. Murphy, A. Hafner, I. S. Cinquini, C. A. Walker, A. N. Boettiger, *Nature* **2019**, *568*, 49.
- [84] M. Liu, Y. Lu, B. Yang, Y. Chen, J. S. D. Radda, M. Hu, S. G. Katz, S. Wang, *Nat. Commun.* **2020**, *11*, 2907.
- [85] J.-H. Su, P. Zheng, S. S. Kinrot, B. Bintu, X. Zhuang, *Cell* **2020**, *182*, 1641.
- [86] Y. Takei, J. Yun, S. Zheng, N. Ollikainen, N. Pierson, J. White, S. Shah, J. Thomassie, S. Suo, C.-H. L. Eng, M. Guttman, G.-C. Yuan, L. Cai, *Nature* **2021**, *590*, 344.
- [87] H. Q. Nguyen, S. Chatteraj, D. Castillo, S. C. Nguyen, G. Nir, A. Lioutas, E. A. Hershberg, N. M. C. Martins, P. L. Reginato, M. Hannan, B. J. Beliveau, G. M. Church, E. R. Daugharty, M. A. Marti-Renom, C.-T. Wu, *Nat. Methods* **2020**, *17*, 822.
- [88] A. C. Payne, Z. D. Chiang, P. L. Reginato, S. M. Mangiameli, E. M. Murray, C.-C. Yao, S. Markoulaki, A. S. Earl, A. S. Labade, R. Jaenisch, G. M. Church, E. S. Boyden, J. D. Buenrostro, F. Chen, *Science* **2021**, *371*, eaay3446.
- [89] J. D. Buenrostro, P. G. Giresi, L. C. Zaba, H. Y. Chang, W. J. Greenleaf, *Nat. Methods* **2013**, *10*, 1213.
- [90] J. D. Buenrostro, B. Wu, U. M. Litzenburger, D. Ruff, M. L. Gonzales, M. P. Snyder, H. Y. Chang, W. J. Greenleaf, *Nature* **2015**, *523*, 486.
- [91] X. Chen, Y. Shen, W. Draper, J. D. Buenrostro, U. Litzenburger, S. W. Cho, A. T. Satpathy, A. C. Carter, R. P. Ghosh, A. East-Seletsky, J. A. Doudna, W. J. Greenleaf, J. T. Liphardt, H. Y. Chang, *Nat. Methods* **2016**, *13*, 1013.
- [92] C. A. Thornton, R. M. Mulqueen, K. A. Torkenczy, A. Nishida, E. G. Lowenstein, A. J. Fields, F. J. Steemers, W. Zhang, H. L. McConnell, R. L. Woltjer, A. Mishra, K. M. Wright, A. C. Adey, *Nat. Commun.* **2021**, *12*, 1274.
- [93] E. Llorens-Bobadilla, M. Zamboni, M. Marklund, N. Bhalla, X. Chen, J. Hartman, J. Frisé, P. L. Ståhl, *Nat. Biotechnol.* **2023**, *41*, 1085.
- [94] Y. Deng, M. Bartosovic, S. Ma, D. Zhang, P. Kukanja, Y. Xiao, G. Su, Y. Liu, X. Qin, G. B. Rosoklija, A. J. Dwork, J. J. Mann, M. L. Xu, S. Halene, J. E. Craft, K. W. Leong, M. Boldrini, G. Castelo-Branco, R. Fan, *Nature* **2022**, *609*, 375.
- [95] S. M. Mangiameli, H. Chen, A. S. Earl, J. A. Dobkin, D. Lesman, J. D. Buenrostro, F. Chen, *Nat. Methods* **2023**, *20*, 686.
- [96] Y. Deng, M. Bartosovic, P. Kukanja, D. Zhang, Y. Liu, G. Su, A. Enniful, Z. Bai, G. Castelo-Branco, R. Fan, *Science* **2022**, *375*, 681.
- [97] Z. Liu, C. Deng, Z. Zhou, Y. Xiao, S. Jiang, B. Zhu, L. B. Naler, X. Jia, D. D. Yao, C. Lu, *Cell Rep. Methods* **2024**, *4*, 100738.
- [98] Z. Cao, C. Chen, B. He, K. Tan, C. Lu, *Nat. Methods* **2015**, *12*, 959.
- [99] X. Ren, R. Deng, K. Zhang, Y. Sun, Y. Li, J. Li, *Angew. Chem. Int. Ed Engl.* **2021**, *60*, 22646.
- [100] Y. Ma, W. Guo, Q. Mou, X. Shao, M. Lyu, V. Garcia, L. Kong, W. Lewis, C. Ward, Z. Yang, X. Pan, S. S. Yi, Y. Lu, *Nat. Biotechnol.* **2024**, *42*, 608.
- [101] S. S. Rubakhin, E. V. Romanova, P. Nemes, J. V. Sweedler, *Nat. Methods* **2011**, *8*, S20.
- [102] A. A. Santos, T. C. Delgado, V. Marques, C. Ramirez-Moncayo, C. Alonso, A. Vidal-Puig, Z. Hall, M. L. Martínez-Chantar, C. M. P. Rodrigues, *Hepatology* **2024**, *79*, 1158.
- [103] R. Ait-Belkacem, L. Sellami, C. Villard, E. DePauw, D. Calligaris, D. Lafitte, *Trends Biotechnol.* **2012**, *30*, 466.
- [104] S. Ganesh, T. Hu, E. Woods, M. Allam, S. Cai, W. Henderson, A. F. Coskun, *Sci. Adv.* **2021**, *7*, eabd0957.
- [105] D. Briggs, *Surf. Interface Anal.* **1983**, *5*, 113.
- [106] R. M. Caprioli, T. B. Farmer, J. Gile, *Anal. Chem.* **1997**, *69*, 4751.
- [107] Z. Takáts, J. M. Wiseman, B. Gologan, R. G. Cooks, *Science* **2004**, *306*, 471.
- [108] M. A. Brunet, M. L. Kraft, *Acc. Chem. Res.* **2023**, *56*, 752.
- [109] J.-N. Audinot, P. Philipp, O. De Castro, A. Biesemeier, Q. H. Hoang, T. Wirtz, *Rep. Prog. Phys.* **2021**, *84*, 105901.
- [110] A. M. Belu, D. J. Graham, D. G. Castner, *Biomaterials* **2003**, *24*, 3635.
- [111] D. S. Cornett, M. L. Reyzer, P. Chaurand, R. M. Caprioli, *Nat. Methods* **2007**, *4*, 828.
- [112] L. Li, R. W. Garden, J. V. Sweedler, *Trends Biotechnol.* **2000**, *18*, 151.
- [113] T. Bien, K. Koerfer, J. Schwenzfeier, K. Dreisewerd, J. Soltwisch, *Proc. Natl. Acad. Sci. USA* **2022**, *119*, 2114365119.
- [114] L. Capolupo, I. Khven, A. R. Lederer, L. Mazzeo, G. Glousker, S. Ho, F. Russo, J. P. Montoya, D. R. Bhandari, A. P. Bowman, S. R. Ellis, R. Guiet, O. Burri, J. Detzner, J. Muthing, K. Homiczko, F. Kuonen, M. Gilliet, B. Spengler, R. M. A. Heeren, G. P. Dotto, G. La Manno, G. D'Angelo, *Science* **2022**, *376*, eabh1623.
- [115] R. G. Cooks, Z. Ouyang, Z. Takats, J. M. Wiseman, *Science* **2006**, *311*, 1566.
- [116] N. M. Morato, R. G. Cooks, *Acc. Chem. Res.* **2023**, *56*, 2526.
- [117] J. Y. Kishi, S. W. Lapan, B. J. Beliveau, E. R. West, A. Zhu, H. M. Sasaki, S. K. Saka, Y. Wang, C. L. Cepko, P. Yin, *Nat. Methods* **2019**, *16*, 533.
- [118] F. Jiang, X. Zhou, Y. Qian, M. Zhu, L. Wang, Z. Li, Q. Shen, M. Wang, F. Qu, G. Cui, K. Chen, G. Peng, *Nat. Methods* **2023**, *20*, 1048.
- [119] Y. Liu, M. DiStasio, G. Su, H. Asashima, A. Enniful, X. Qin, Y. Deng, J. Nam, F. Gao, P. Bordignon, M. Cassano, M. Tomayko, M. Xu, S. Halene, J. E. Craft, D. Hafler, R. Fan, *Nat. Biotechnol.* **2023**, *41*, 1405.

- [120] N. Ben-Chetrit, X. Niu, A. D. Swett, J. Sotelo, M. S. Jiao, C. M. Stewart, C. Potenski, P. Mielinis, P. Roelli, M. Stoeckius, D. A. Landau, *Nat. Biotechnol.* **2023**, *41*, 788.
- [121] S. Vickovic, B. Lötstedt, J. Klughammer, S. Mages, A. Segerstolpe, O. Rozenblatt-Rosen, A. Regev, *Nat. Commun.* **2022**, *13*, 795.
- [122] S. Liao, Y. Heng, W. Liu, J. Xiang, Y. Ma, L. Chen, X. Feng, D. Jia, D. Liang, C. Huang, J. Zhang, M. Jian, K. Su, M. Li, Y.-H. Loh, A. Chen, X. Xu, *bioRxiv* **2023**, 538364.
- [123] H. Zeng, J. Huang, H. Zhou, W. J. Meilandt, B. Dejanovic, Y. Zhou, C. J. Bohlen, S.-H. Lee, J. Ren, A. Liu, Z. Tang, H. Sheng, J. Liu, M. Sheng, X. Wang, *Nat. Neurosci.* **2023**, *26*, 430.
- [124] X. Wu, W. Xu, L. Deng, Y. Li, Z. Wang, L. Sun, A. Gao, H. Wang, X. Yang, C. Wu, Y. Zou, K. Yan, Z. Liu, L. Zhang, G. Du, L. Yang, D. Lin, J. Yue, P. Wang, Y. Han, Z. Fu, J. Dai, G. Cao, *Nat. Biomed. Eng.* **2024**, *8*, 872.
- [125] T. Vu, A. Vallmitjana, J. Gu, K. La, Q. Xu, J. Flores, J. Zimak, J. Shiu, L. Hosohama, J. Wu, C. Douglas, M. L. Waterman, A. Ganesan, P. N. Hedde, E. Gratton, W. Zhao, *Nat. Commun.* **2022**, *13*, 169.
- [126] C. Ortiz, M. Carlen, K. Meletis, *Annu. Rev. Neurosci.* **2021**, *44*, 547.
- [127] E. S. Lein, M. J. Hawrylycz, N. Ao, M. Ayres, A. Bensinger, A. Bernard, A. F. Boe, M. S. Boguski, K. S. Brockway, E. J. Byrnes, L. Chen, L. Chen, T.-M. Chen, M. C. Chin, J. Chong, B. E. Crook, A. Czaplinska, C. N. Dang, S. Datta, N. R. Dee, A. L. Desaki, T. Desta, E. Diep, T. A. Dolbeare, M. J. Donelan, H.-W. Dong, J. G. Dougherty, B. J. Duncan, A. J. Ebbert, G. Eichele, et al., *Nature* **2007**, *445*, 168.
- [128] C. Ortiz, J. F. Navarro, A. Jurek, A. Märtin, J. Lundeberg, K. Meletis, *Sci. Adv.* **2020**, *6*, eabb3446.
- [129] M. Zhang, X. Pan, W. Jung, A. R. Halpern, S. W. Eichhorn, Z. Lei, L. Cohen, K. A. Smith, B. Tasic, Z. Yao, H. Zeng, X. Zhuang, *Nature* **2023**, *624*, 343.
- [130] Z. Yao, C. T. J. van Velthoven, M. Kunst, M. Zhang, D. McMillen, C. Lee, W. Jung, J. Goldy, A. Abdelhak, M. Aitken, K. Baker, P. Baker, E. Barkan, D. Bertagnolli, A. Bhandiwad, C. Bielsstein, P. Bishwakarma, J. Campos, D. Carey, T. Casper, A. B. Chakka, R. Chakrabarty, S. Chavan, M. Chen, M. Clark, J. Close, K. Crichton, S. Daniel, P. DiValentin, T. Dolbeare, et al., *Nature* **2023**, *624*, 317.
- [131] J. Langlieb, N. S. Sachdev, K. S. Balderrama, N. M. Nadaf, M. Raj, E. Murray, J. T. Webber, C. Vanderburg, V. Gazestani, D. Tward, C. Mezas, X. Li, K. Flowers, D. M. Cable, T. Norton, P. Mitra, F. Chen, E. Z. Macosko, *Nature* **2023**, *624*, 333.
- [132] H. Shi, Y. He, Y. Zhou, J. Huang, K. Maher, B. Wang, Z. Tang, S. Luo, P. Tan, M. Wu, Z. Lin, J. Ren, Y. Thapa, X. Tang, K. Y. Chan, B. E. Deverman, H. Shen, A. Liu, J. Liu, X. Wang, *Nature* **2023**, *622*, 552.
- [133] X. Chen, S. Fischer, M. C. P. Rue, A. Zhang, D. Mukherjee, P. O. Kanold, J. Gillis, A. M. Zador, *Nature* **2024**, E1.
- [134] D. J. Di Bella, E. Habibi, R. R. Stickels, G. Scalia, J. Brown, P. Yadollahpour, S. M. Yang, C. Abbate, T. Biancalani, E. Z. Macosko, F. Chen, A. Regev, P. Arlotta, *Nature* **2021**, *595*, 554.
- [135] R. Fang, C. Xia, J. L. Close, M. Zhang, J. He, Z. Huang, A. R. Halpern, B. Long, J. A. Miller, E. S. Lein, X. Zhuang, *Science* **2022**, *377*, 56.
- [136] M. Zhang, S. W. Eichhorn, B. Zingg, Z. Yao, K. Cotter, H. Zeng, H. Dong, X. Zhuang, *Nature* **2021**, *598*, 137.
- [137] BRAIN Initiative Cell Census Network (BICCN), *Nature* **2021**, *598*, 86.
- [138] A. S. Boeshaghi, Z. Yao, C. van Velthoven, K. Smith, B. Tasic, H. Zeng, L. Pachter, *Nature* **2021**, *598*, 195.
- [139] J. R. Moffitt, D. Bambach-Mukku, S. W. Eichhorn, E. Vaughn, K. Shekhar, J. D. Perez, N. D. Rubinstein, J. Hao, A. Regev, C. Dulac, X. Zhuang, *Science* **2018**, *362*, eaau5324.
- [140] R. Chen, T. R. Blosser, M. N. Djekidel, J. Hao, A. Bhattacharjee, W. Chen, L. M. Tuesta, X. Zhuang, Y. Zhang, *Nat. Neurosci.* **2021**, *24*, 1757.
- [141] K. R. Maynard, L. Collado-Torres, L. M. Weber, C. Uyttingco, B. K. Barry, S. R. Williams, J. L. Cattalini2nd, M. N. Tran, Z. Besich, M. Tippi, J. Chew, Y. Yin, J. E. Kleinman, T. M. Hyde, N. Rao, S. C. Hicks, K. Martinowich, A. E. Jaffe, *Nat. Neurosci.* **2021**, *24*, 425.
- [142] J. M. Kechschull, E. B. Richman, N. Ringach, D. Friedmann, E. Albarran, S. S. Kolluru, R. C. Jones, W. E. Allen, Y. Wang, S. W. Cho, H. Zhou, J. B. Ding, H. Y. Chang, K. Deisseroth, S. R. Quake, L. Luo, *Science* **2020**, *370*.
- [143] J. A. Stogsdill, K. Kim, L. Binan, S. L. Farhi, J. Z. Levin, P. Arlotta, *Nature* **2022**, *608*, 750.
- [144] Y. Takei, S. Zheng, J. Yun, S. Shah, N. Pierson, J. White, S. Schindler, C. H. Tischbirek, G.-C. Yuan, L. Cai, *Science* **2021**, *374*, 586.
- [145] H. Liu, Q. Zeng, J. Zhou, A. Bartlett, B.-A. Wang, P. Berube, W. Tian, M. Kenworthy, J. Altshul, J. R. Nery, H. Chen, R. G. Castanon, S. Zu, Y. E. Li, J. Lucero, J. K. Osteen, A. Pinto-Duarte, J. Lee, J. Rink, S. Cho, N. Emerson, M. Nunn, C. O'Connor, Z. Wu, I. Stoica, Z. Yao, K. A. Smith, B. Tasic, C. Luo, J. R. Dixon, et al., *Nature* **2023**, *624*, 366.
- [146] Q. Li, Z. Lin, R. Liu, X. Tang, J. Huang, Y. He, X. Sui, W. Tian, H. Shen, H. Zhou, H. Sheng, H. Shi, L. Xiao, X. Wang, J. Liu, *Cell* **2023**, *186*, 2002.
- [147] S. W. Oh, J. A. Harris, L. Ng, B. Winslow, N. Cain, S. Mihalas, Q. Wang, C. Lau, L. Kuan, A. M. Henry, M. T. Mortrud, B. Ouellette, T. N. Nguyen, S. A. Sorensen, C. R. Slaughterbeck, W. Wakeman, Y. Li, D. Feng, A. Ho, E. Nicholas, K. E. Hirokawa, P. Bohn, K. M. Joines, H. Peng, M. J. Hawrylycz, J. W. Phillips, J. G. Hohmann, P. Wohnoutka, C. R. Gerfen, C. Koch, et al., *Nature* **2014**, *508*, 207.
- [148] Z. J. Huang, *Neuron* **2014**, *83*, 1284.
- [149] I. R. Wickersham, S. Finke, K.-K. Conzelmann, E. M. Callaway, *Nat. Methods* **2007**, *4*, 47.
- [150] I. R. Wickersham, D. C. Lyon, R. J. O. Barnard, T. Mori, S. Finke, K.-K. Conzelmann, J. A. T. Young, E. M. Callaway, *Neuron* **2007**, *53*, 639.
- [151] Y. Qian, J. Li, S. Zhao, E. A. Matthews, M. Adoff, W. Zhong, X. An, M. Yeo, C. Park, X. Yang, B.-S. Wang, D. G. Southwell, Z. J. Huang, *Nature* **2022**, *610*, 713.
- [152] J. Livet, T. A. Weissman, H. Kang, R. W. Draft, J. Lu, R. A. Bennis, J. R. Sanes, J. W. Lichtman, *Nature* **2007**, *450*, 56.
- [153] J. M. Kechschull, P. Garcia da Silva, A. P. Reid, I. D. Peikon, D. F. Albeanu, A. M. Zador, *Neuron* **2016**, *91*, 975.
- [154] X. Chen, Y.-C. Sun, H. Zhan, J. M. Kechschull, S. Fischer, K. Matho, Z. J. Huang, J. Gillis, A. M. Zador, *Cell* **2019**, *179*, 772.
- [155] Y.-C. Sun, X. Chen, S. Fischer, S. Lu, H. Zhan, J. Gillis, A. M. Zador, *Nat. Neurosci.* **2021**, *24*, 873.
- [156] Y. Chen, X. Chen, B. Baserdem, H. Zhan, Y. Li, M. B. Davis, J. M. Kechschull, A. M. Zador, A. A. Koulakov, D. F. Albeanu, *Cell* **2022**, *185*, 4117.
- [157] S. Bugeon, J. Duffield, M. Dipoppa, A. Ritoux, I. Prankerd, D. Nicoloutsopoulos, D. Orme, M. Shinn, H. Peng, H. Forrest, A. Viduolyte, C. B. Reddy, Y. Isogai, M. Carandini, K. D. Harris, *Nature* **2022**, *607*, 330.
- [158] Y. Vanrobaeys, U. Mukherjee, L. Langmack, S. E. Beyer, E. Bahl, L.-C. Lin, J. J. Michaelson, T. Abel, S. Chatterjee, *Nat. Commun.* **2023**, *14*, 6100.
- [159] W. Sun, Z. Liu, X. Jiang, M. B. Chen, H. Dong, J. Liu, T. C. Südhof, S. R. Quake, *Nature* **2024**, *627*, 374.
- [160] J. A. Osterhout, V. Kapoor, S. W. Eichhorn, E. Vaughn, J. D. Moore, D. Liu, D. Lee, L. A. DeNardo, L. Luo, X. Zhuang, C. Dulac, *Nature* **2022**, *606*, 937.
- [161] I.-H. Wang, E. Murray, G. Andrews, H.-C. Jiang, S. J. Park, E. Donnard, V. Durán-Laforet, D. M. Bear, T. E. Faust, M. Garber, C. E. Baer, D. P. Schafer, Z. Weng, F. Chen, E. Z. Macosko, P. L. Greer, *Nat. Neurosci.* **2022**, *25*, 484.
- [162] S. Xu, H. Yang, V. Menon, A. L. Lemire, L. Wang, F. E. Henry, S. C. Turaga, S. M. Sternson, *Science* **2020**, *370*, eabb2494.
- [163] M. Kampmann, *Nat. Rev. Neurosci.* **2024**, *25*, 351.
- [164] S. Maniatis, T. Åijö, S. Vickovic, C. Braine, K. Kang, A. Mollbrink, D. Fagegaltier, Ž. Andrusivová, S. Saarenpää, G. Saiz-Castro,

- M. Cuevas, A. Watters, J. Lundeberg, R. Bonneau, H. Phatnani, *Science* **2019**, 364, 89.
- [165] M. Kaufmann, A.-L. Schaupp, R. Sun, F. Coscia, C. A. Dendrou, A. Cortes, G. Kaur, H. G. Evans, A. Mollbrink, J. F. Navarro, J. K. Sonner, C. Mayer, G. C. DeLuca, J. Lundeberg, P. M. Matthews, K. E. Attfield, M. A. Friese, M. Mann, L. Fugger, *Nat. Neurosci.* **2022**, 25, 944.
- [166] W.-T. Chen, A. Lu, K. Craessaerts, B. Pavie, C. Sala Frigerio, N. Corthout, X. Qian, J. Laláková, M. Kühnemund, I. Voytyuk, L. Wolfs, R. Mancuso, E. Salta, S. Balusu, A. Snellinx, S. Munck, A. Jurek, J. F. Navarro, T. C. Saido, I. Huitinga, J. Lundeberg, M. Fiers, B. De Strooper, *Cell* **2020**, 182, 976.
- [167] J. I. Wood, E. Wong, R. Joghee, A. Balbaa, K. S. Vitanova, K. M. Stringer, A. Vanshojack, S.-L. J. Phelan, F. Launchbury, S. Desai, T. Tripathi, J. Hanrieder, D. M. Cummings, J. Hardy, F. A. Edwards, *Cell Rep.* **2022**, 41, 111686.
- [168] J. M. Walker, M. E. Orr, T. C. Orr, E. L. Thorn, T. D. Christie, R. T. Yokoda, M. Vij, A. J. Ehrenberg, G. A. Marx, A. T. McKenzie, J. Kauffman, E. Selmanovic, T. Wisniewski, E. Drummond, C. L. White3rd, J. F. Cray, K. Farrell, T. F. Kautz, E. V. Daoud, T. E. Richardson, *Alzheimers. Dement.* **2024**, 20, 783.
- [169] M. Y. Batiuk, T. Tyler, K. Dragicevic, S. Mei, R. Rydbirk, V. Petukhov, R. Deviatiiarov, D. Sedmak, E. Frank, V. Feher, N. Habek, Q. Hu, A. Igolkina, L. Roszik, U. Pfisterer, D. Garcia-Gonzalez, Z. Petanjek, I. Adorjan, P. V. Kharchenko, K. Khodosevich, *Sci. Adv.* **2022**, 8, eabn8367.
- [170] A. E. Jaffe, D. J. Hoepfner, T. Saito, L. Blanpain, J. Ukaigwe, E. E. Burke, L. Collado-Torres, R. Tao, K. Tajinda, K. R. Maynard, M. N. Tran, K. Martinowich, A. Deep-Soboslay, J. H. Shin, J. E. Kleinman, D. R. Weinberger, M. Matsumoto, T. M. Hyde, *Nat. Neurosci.* **2020**, 23, 510.
- [171] D. Ya, Y. Zhang, Q. Cui, Y. Jiang, J. Yang, N. Tian, W. Xiang, X. Lin, Q. Li, R. Liao, *Front Cell Dev Biol* **2023**, 11, 1142923.
- [172] H.-E. Park, S. H. Jo, R. H. Lee, C. P. Macks, T. Ku, J. Park, C. W. Lee, J. K. Hur, C. H. Sohn, *Adv. Sci.* **2023**, 10, 2206939.
- [173] N. Jung, T.-K. Kim, *Exp. Mol. Med.* **2023**, 55, 2105.
- [174] J. Cao, M. Spielmann, X. Qiu, X. Huang, D. M. Ibrahim, A. J. Hill, F. Zhang, S. Mundlos, L. Christiansen, F. J. Steemers, C. Trapnell, J. Shendure, *Nature* **2019**, 566, 496.
- [175] M. E. Dickinson, The International Mouse Phenotyping Consortium, A. M. Flenniken, X. Ji, L. Teboul, M. D. Wong, J. K. White, T. F. Meehan, W. J. Weninger, H. Westerberg, H. Adissu, C. N. Baker, L. Bower, J. M. Brown, L. B. Caddle, F. Chiani, D. Clary, J. Cleak, M. J. Daly, J. M. Denegre, B. Doe, M. E. Dolan, S. M. Edie, H. Fuchs, V. Gailus-Durner, A. Galli, A. Gambadoro, J. Gallegos, S. Guo, N. R. Horner, C.-W. Hsu, et al., *Nature* **2016**, 537, 508.
- [176] M. Huch, B.-K. Koo, *Development* **2015**, 142, 3113.
- [177] T. Lohoff, S. Ghazanfar, A. Missarova, N. Koulina, N. Pierson, J. A. Griffiths, E. S. Bardot, C.-H. L. Eng, R. C. V. Tyser, R. Argelaguet, C. Guibentif, S. Srinivas, J. Briscoe, B. D. Simons, A.-K. Hadjantonakis, B. Göttgens, W. Reik, J. Nichols, L. Cai, J. C. Marioni, *Nat. Biotechnol.* **2022**, 40, 74.
- [178] A. S. Kumar, L. Tian, A. Bolondi, A. A. Hernández, R. Stickels, H. Kretzmer, E. Murray, L. Wittler, M. Walther, G. Barakat, L. Haut, Y. Elkabetz, E. Z. Macosko, L. Guignard, F. Chen, A. Meissner, *Nat. Genet.* **2023**, 55, 1176.
- [179] F. Qu, W. Li, J. Xu, R. Zhang, J. Ke, X. Ren, X. Meng, L. Qin, J. Zhang, F. Lu, X. Zhou, X. Luo, Z. Zhang, M. Wang, G. Wu, D. Pei, J. Chen, G. Cui, S. Suo, G. Peng, *Nat. Commun.* **2023**, 14, 4599.
- [180] J. O. Piña, R. Raju, D. M. Roth, E. W. Winchester, P. Chattaraj, F. Kidwai, F. R. Fauz, J. Iben, A. Mitra, K. Campbell, G. Fridell, C. Esnault, J. L. Cotney, R. K. Dale, R. N. D'Souza, *Nat. Commun.* **2023**, 14, 5687.
- [181] G. L. a. Manno, K. Siletti, A. Furlan, D. Gyllborg, E. Vinsland, A. Mossi Albiach, C. Mattsson Langseth, I. Khven, A. R. Lederer, L. M. Dratva, A. Johnsson, M. Nilsson, P. Lönnerberg, S. Linnarsson, *Nature* **2021**, 596, 92.
- [182] S. Bastide, E. Chomsky, B. Saudemont, Y. Loe-Mie, S. Schmutz, S. Novault, H. Marlow, A. Tanay, F. Spitz, *Sci. Adv.* **2022**, 8, eadd0695.
- [183] C. D. Allis, T. Jenuwein, *Nat. Rev. Genet.* **2016**, 17, 487.
- [184] M. Asp, S. Giacomello, L. Larsson, C. Wu, D. Fürth, X. Qian, E. Wårdell, J. Custodio, J. Reimegård, F. Salmén, C. Österholm, P. L. Ståhl, E. Sundström, E. Åkesson, O. Bergmann, M. Bienko, A. Månsson-Broberg, M. Nilsson, C. Sylvén, J. Lundeberg, *Cell* **2019**, 179, 1647.
- [185] E. N. Farah, R. K. Hu, C. Kern, Q. Zhang, T.-Y. Lu, Q. Ma, S. Tran, B. Zhang, D. Carlin, A. Monell, A. P. Blair, Z. Wang, J. Eschbach, B. Li, E. Destici, B. Ren, S. M. Evans, S. Chen, Q. Zhu, N. C. Chi, *Nature* **2024**, 627, 854.
- [186] O. E. Olaniru, U. Kadolsky, S. Kannambath, H. Vaikkinen, K. Fung, P. Dhami, S. J. Persaud, *Cell Metab.* **2023**, 35, 184.
- [187] B. Zhang, P. He, J. E. G. Lawrence, S. Wang, E. Tuck, B. A. Williams, K. Roberts, V. Kleshchevnikov, L. Mamanova, L. Bolt, K. Polanski, T. Li, R. Elmentaite, E. S. Fasouli, M. Prete, X. He, N. Yayon, Y. Fu, H. Yang, C. Liang, H. Zhang, R. Blain, A. Chedotal, D. R. FitzPatrick, H. Firth, A. Dean, O. A. Bayraktar, J. C. Marioni, R. A. Barker, M. A. Storer, et al., *Nature* **2024**, 635, 668.
- [188] X. Li, Z. Andrusivova, P. Czarnewski, C. M. Langseth, A. Andersson, Y. Liu, D. Gyllborg, E. Braun, L. Larsson, L. Hu, Z. Alekseenko, H. Lee, C. Avenel, H. K. Kallner, E. Åkesson, I. Adameyko, M. Nilsson, S. Linnarsson, J. Lundeberg, E. Sundström, *Nat. Neurosci.* **2023**, 26, 891.
- [189] S. Gribaudo, R. Robert, B. van Sambeek, C. Mirdass, A. Lyubimova, K. Bouhali, J. Ferent, X. Morin, A. van Oudenaarden, S. Nedelec, *Nat. Biotechnol.* **2024**, 42, 1243.
- [190] Y. Li, Z. Li, C. Wang, M. Yang, Z. He, F. Wang, Y. Zhang, R. Li, Y. Gong, B. Wang, B. Fan, C. Wang, L. Chen, H. Li, P. Shi, N. Wang, Z. Wei, Y.-L. Wang, L. Jin, P. Du, J. Dong, J. Jiao, *Cell* **2023**, 186, 5892.
- [191] K. Holler, A. Neuschulz, P. Drewe-Boß, J. Mintcheva, B. Spanjaard, R. Arsie, U. Ohler, M. Landthaler, J. P. Junker, *Nat. Commun.* **2021**, 12, 3358.
- [192] C. Liu, R. Li, Y. Li, X. Lin, K. Zhao, Q. Liu, S. Wang, X. Yang, X. Shi, Y. Ma, C. Pei, H. Wang, W. Bao, J. Hui, T. Yang, Z. Xu, T. Lai, M. A. Berberoglu, S. K. Sahu, M. A. Esteban, K. Ma, G. Fan, Y. Li, S. Liu, A. Chen, X. Xu, Z. Dong, L. Liu, *Dev. Cell* **2022**, 57, 1284.
- [193] M. Wang, Q. Hu, T. Lv, Y. Wang, Q. Lan, R. Xiang, Z. Tu, Y. Wei, K. Han, C. Shi, J. Guo, C. Liu, T. Yang, W. Du, Y. An, M. Cheng, J. Xu, H. Lu, W. Li, S. Zhang, A. Chen, W. Chen, Y. Li, X. Wang, X. Xu, Y. Hu, L. Liu, *Dev. Cell* **2022**, 57, 1271.
- [194] X. Wei, S. Fu, H. Li, Y. Liu, S. Wang, W. Feng, Y. Yang, X. Liu, Y.-Y. Zeng, M. Cheng, Y. Lai, X. Qiu, L. Wu, N. Zhang, Y. Jiang, J. Xu, X. Su, C. Peng, L. Han, W. P.-K. Lou, C. Liu, Y. Yuan, K. Ma, T. Yang, X. Pan, S. Gao, A. Chen, M. A. Esteban, H. Yang, J. Wang, et al., *Science* **2022**, 377, eabp9444.
- [195] Y. Kojima, O. H. Tam, P. P. L. Tam, *Semin. Cell Dev. Biol.* **2014**, 34, 65.
- [196] L. Solnica-Krezel, D. S. Sepich, *Annu. Rev. Cell Dev. Biol.* **2012**, 28, 687.
- [197] G. Peng, S. Suo, J. Chen, W. Chen, C. Liu, F. Yu, R. Wang, S. Chen, N. Sun, G. Cui, L. Song, P. P. L. Tam, J.-D. J. Han, N. Jing, *Dev. Cell* **2016**, 36, 681.
- [198] G. Peng, S. Suo, G. Cui, F. Yu, R. Wang, J. Chen, S. Chen, Z. Liu, G. Chen, Y. Qian, P. P. L. Tam, J.-D. J. Han, N. Jing, *Nature* **2019**, 572, 528.
- [199] Y. He, X. Tang, J. Huang, J. Ren, H. Zhou, K. Chen, A. Liu, H. Shi, Z. Lin, Q. Li, A. Aditham, J. Ounadjela, E. I. Grody, J. Shu, J. Liu, X. Wang, *Nat. Commun.* **2021**, 12, 5909.

- [200] G. Cui, S. Feng, Y. Yan, L. Wang, X. He, X. Li, Y. Duan, J. Chen, K. Tang, P. Zheng, P. P. L. Tam, W. Si, N. Jing, G. Peng, *Cell Rep.* **2022**, *40*, 111285.
- [201] Z. Xiao, L. Cui, Y. Yuan, N. He, X. Xie, S. Lin, X. Yang, X. Zhang, P. Shi, Z. Wei, Y. Li, H. Wang, X. Wang, Y. Wei, J. Guo, L. Yu, *Cell* **2024**, *187*, 2855.
- [202] R. Vento-Tormo, M. Efremova, R. A. Botting, M. Y. Turco, M. Vento-Tormo, K. B. Meyer, J.-E. Park, E. Stephenson, K. Polański, A. Goncalves, L. Gardner, S. Holmqvist, J. Henriksson, A. Zou, A. M. Sharkey, B. Millar, B. Innes, L. Wood, A. Wilbrey-Clark, R. P. Payne, M. A. Ivarsson, S. Lisgo, A. Filby, D. H. Rowitch, J. N. Bulmer, G. J. Wright, M. J. T. Stubbington, M. Haniffa, A. Moffett, S. A. Teichmann, *Nature* **2018**, *563*, 347.
- [203] R. Pijnenborg, L. Vercruyse, M. Hanssens, *Placenta* **2006**, *27*, 939.
- [204] A. Arutyunyan, K. Roberts, K. Troulé, F. C. K. Wong, M. A. Sheridan, I. Kats, L. Garcia-Alonso, B. Velten, R. Hoo, E. R. Ruiz-Morales, C. Sancho-Serra, J. Shilts, L.-F. Handfield, L. Marconato, E. Tuck, L. Gardner, C. I. Mazzeo, Q. Li, I. Kelava, G. J. Wright, E. Prigmore, S. A. Teichmann, O. A. Bayraktar, A. Moffett, O. Stegle, M. Y. Turco, R. Vento-Tormo, *Nature* **2023**, *616*, 143.
- [205] S. Greenbaum, I. Averbukh, E. Soon, G. Rizzuto, A. Baranski, N. F. Greenwald, A. Kagel, M. Bosse, E. G. Jaswa, Z. Khair, S. Kwok, S. Warshawsky, H. Piyadasa, M. Goldston, A. Spence, G. Miller, M. Schwartz, W. Graf, D. Van Valen, V. D. Winn, T. Hollmann, L. Keren, M. van de Rijn, M. Angelo, *Nature* **2023**, *619*, 595.
- [206] M. A. Lancaster, M. Renner, C.-A. Martin, D. Wenzel, L. S. Bicknell, M. E. Hurles, T. Homfray, J. M. Penninger, A. P. Jackson, J. A. Knoblich, *Nature* **2013**, *501*, 373.
- [207] A. Uzquiano, A. J. Kedaigle, M. Pignoni, B. Paulsen, X. Adiconis, K. Kim, T. Faits, S. Nagaraja, N. Antón-Bolaños, C. Gerhardinger, A. Tucewicz, E. Murray, X. Jin, J. Buenrostro, F. Chen, S. Velasco, A. Regev, J. Z. Levin, P. Arlotta, *Cell* **2022**, *185*, 3770.
- [208] S. Wang, C.-W. Lin, A. E. Carleton, C. L. Cortez, C. Johnson, L. E. Taniguchi, N. Sekulovski, R. F. Townshend, V. Basrur, A. I. Nesvizhskii, P. Zou, J. Fu, D. L. Gumucio, M. C. Duncan, K. Taniguchi, *Sci. Adv.* **2021**, *7*.
- [209] P. Wahle, G. Brancati, C. Harmel, Z. He, G. Gut, J. S. Del Castillo, A. Xavier da Silveira Dos Santos, Q. Yu, P. Noser, J. S. Fleck, B. Gjeta, D. Pavlinić, S. Picelli, M. Hess, G. W. Schmidt, T. T. A. Lummen, Y. Hou, P. Galliker, D. Goldblum, M. Balogh, C. S. Cowan, H. P. N. Scholl, B. Roska, M. Renner, L. Pelkmans, B. Treutlein, J. G. Camp, *Nat. Biotechnol.* **2023**, *41*, 1765.
- [210] P. Datlinger, A. F. Rendeiro, C. Schmid, T. Krausgruber, P. Traxler, J. Klughammer, L. C. Schuster, A. Kuchler, D. Alpar, C. Bock, *Nat. Methods* **2017**, *14*, 297.
- [211] I. Legnini, L. Emmenegger, A. Zappulo, A. Rybak-Wolf, R. Wurmus, A. O. Martinez, C. C. Jara, A. Boltengagen, T. Hessler, G. Mastrobuoni, S. Kempa, R. Zinzen, A. Woehler, N. Rajewsky, *Nat. Methods* **2023**, *20*, 1544.
- [212] V. Gorgoulis, P. D. Adams, A. Alimonti, D. C. Bennett, O. Bischof, C. Bishop, J. Campisi, M. Collado, K. Evangelou, G. Ferbeyre, J. Gil, E. Hara, V. Krizhanovsky, D. Jurk, A. B. Maier, M. Narita, L. Niedernhofer, J. F. Passos, P. D. Robbins, C. A. Schmitt, J. Sedivy, K. Vougas, T. von Zglinicki, D. Zhou, M. Serrano, M. Demaria, *Cell* **2019**, *179*, 813.
- [213] A. U. Gurkar, A. A. Gerencser, A. L. Mora, A. C. Nelson, A. R. Zhang, A. B. Lagnado, A. Enniful, C. Benz, D. Furman, D. Beaulieu, D. Jurk, E. L. Thompson, F. Wu, F. Rodriguez, G. Barthel, H. Chen, H. Phatnani, I. Heckenbach, J. H. Chuang, J. Horrell, J. Petrescu, J. K. Alder, J. H. Lee, L. J. Niedernhofer, M. Kumar, M. Königshoff, M. Bueno, M. Sokka, M. Scheibye-Knudsen, N. Neretti, et al., *Nat. Aging* **2023**, *3*, 776.
- [214] M. Xu, T. Pirtskhalava, J. N. Farr, B. M. Weigand, A. K. Palmer, M. M. Weivoda, C. L. Inman, M. B. Ogrodnik, C. M. Hachfeld, D. G. Fraser, J. L. Onken, K. O. Johnson, G. C. Verzosa, L. G. P. Langhi, M. Weigl, N. Giorgadze, N. K. LeBrasseur, J. D. Miller, D. Jurk, R. J. Singh, D. B. Allison, K. Ejima, G. B. Hubbard, Y. Ikeno, H. Cubro, V. D. Garovic, X. Hou, S. J. Weroha, P. D. Robbins, L. J. Niedernhofer, et al., *Nat. Med.* **2018**, *24*, 1246.
- [215] C. Nikopoulou, N. Kleinenkuhnen, S. Parekh, T. Sandoval, C. Ziegenhain, F. Schneider, P. Giavalisco, K.-F. Donahue, A. J. Vesting, M. Kirchner, M. Bozukova, C. Vossen, J. Altmüller, T. Wunderlich, R. Sandberg, V. Kondylis, A. Tresch, P. Tessarz, *Nat. Aging* **2023**, *3*, 1430.
- [216] W. E. Allen, T. R. Blosser, Z. A. Sullivan, C. Dulac, X. Zhuang, *Cell* **2023**, *186*, 194.
- [217] J. Almagro, H. A. Messal, A. Elosegui-Artola, J. van Rheenen, A. Behrens, *Trends Cancer* **2022**, *8*, 494.
- [218] D. Lähnemann, J. Köster, E. Szczurek, D. J. McCarthy, S. C. Hicks, M. D. Robinson, C. A. Vallejos, K. R. Campbell, N. Beerewinkel, A. Mahfouz, L. Pinello, P. Skums, A. Stamatakis, C. S.-O. Attolini, S. Aparicio, J. Baaijens, M. Balvert, B. de Barbanson, A. Cappuccio, G. Corleone, B. E. Dutilh, M. Florescu, V. Guryev, R. Holmer, K. Jahn, T. J. Lobo, E. M. Keizer, I. Khatiri, S. M. Kielbasa, J. O. Korbel, et al., *Genome Biol.* **2020**, *21*, 31.
- [219] A. C. Anderson, I. Yanai, L. R. Yates, L. Wang, A. Swarbrick, P. Sorger, S. Santagata, W. H. Fridman, Q. Gao, L. Jerby, B. Izar, L. Shang, X. Zhou, *Cancer Cell* **2022**, *40*, 895.
- [220] A. Lomakin, J. Svedlund, C. Strell, M. Gataric, A. Shmatko, G. Rukhovich, J. S. Park, Y. S. Ju, S. Dentro, V. Kleshchevnikov, V. Vaskivskiy, T. Li, O. A. Bayraktar, S. Pinder, A. L. Richardson, S. Santagata, P. J. Campbell, H. Russnes, M. Gerstung, M. Nilsson, L. R. Yates, *Nature* **2022**, *611*, 594.
- [221] J.-R. Lin, S. Wang, S. Coy, Y.-A. Chen, C. Yapp, M. Tyler, M. K. Nariya, C. N. Heiser, K. S. Lau, S. Santagata, P. K. Sorger, *Cell* **2023**, *186*, 363.
- [222] P.-H. Wu, D. M. Gilkes, J. M. Phillip, A. Narkar, T. W.-T. Cheng, J. Marchand, M.-H. Lee, R. Li, D. Wirtz, *Sci. Adv.* **2020**, *6*, eaaw6938.
- [223] V. Marx, *Nat. Methods* **2021**, *18*, 9.
- [224] J. K. Tay, C. Zhu, J. H. Shin, S. X. Zhu, S. Varma, J. W. Foley, S. Vennam, Y. L. Yip, C. K. Goh, D. Y. Wang, K. S. Loh, S. W. Tsao, Q.-T. Le, J. B. Sunwoo, R. B. West, *Sci. Adv.* **2022**, *8*, eabw2445.
- [225] S. Kim, A. C. Lee, H.-B. Lee, J. Kim, Y. Jung, H. S. Ryu, Y. Lee, S. Bae, M. Lee, K. Lee, R. N. Kim, W.-Y. Park, W. Han, S. Kwon, *Genome Biol.* **2018**, *19*, 158.
- [226] J. Kim, S. Kim, H. Yeom, S. W. Song, K. Shin, S. Bae, H. S. Ryu, J. Y. Kim, A. Choi, S. Lee, T. Ryu, Y. Choi, H. Kim, O. Kim, Y. Jung, N. Kim, W. Han, H.-B. Lee, A. C. Lee, S. Kwon, *Nat. Commun.* **2023**, *14*, 5261.
- [227] B. A. Luca, C. B. Steen, M. Matusiak, A. Azizi, S. Varma, C. Zhu, J. Przybyl, A. Espín-Pérez, M. Diehn, A. A. Alizadeh, M. van de Rijn, A. J. Gentles, A. M. Newman, *Cell* **2021**, *184*, 5482.
- [228] S. Tyekucheva, M. Bowden, C. Bango, F. Giunchi, Y. Huang, C. Zhou, A. Bondi, R. Lis, M. Van Hemelrijck, O. Andrés, S.-O. Andersson, R. W. Watson, S. Pennington, S. P. Finn, N. E. Martin, M. J. Stampfer, G. Parmigiani, K. L. Penney, M. Fiorentino, L. A. Mucci, M. Loda, *Nat. Commun.* **2017**, *8*, 420.
- [229] K. Thrane, H. Eriksson, J. Maaskola, J. Hansson, J. Lundeberg, *Cancer Res.* **2018**, *78*, 5970.
- [230] L. Ma, M. O. Hernandez, Y. Zhao, M. Mehta, B. Tran, M. Kelly, Z. Rae, J. M. Hernandez, J. L. Davis, S. P. Martin, D. E. Kleiner, S. M. Hewitt, K. Ylaya, B. J. Wood, T. F. Greten, X. W. Wang, *Cancer Cell* **2019**, *36*, 418.
- [231] M. Janiszewska, L. Liu, V. Almendro, Y. Kuang, C. Paweletz, R. A. Sakr, B. Weigelt, A. B. Hanker, S. Chandarlapaty, T. A. King, J. S. Reis-Filho, C. L. Arteaga, S. Y. Park, F. Michor, K. Polyak, *Nat. Genet.* **2015**, *47*, 1212.

- [232] G. Gambardella, G. Viscido, B. Tumaini, A. Isacchi, R. Bosotti, D. di Bernardo, *Nat. Commun.* **2022**, *13*, 1714.
- [233] H. Liu, A. A. Kiseleva, E. A. Golemis, *Nat. Rev. Cancer* **2018**, *18*, 511.
- [234] Y. Wu, S. Yang, J. Ma, Z. Chen, G. Song, D. Rao, Y. Cheng, S. Huang, Y. Liu, S. Jiang, J. Liu, X. Huang, X. Wang, S. Qiu, J. Xu, R. Xi, F. Bai, J. Zhou, J. Fan, X. Zhang, Q. Gao, *Cancer Discov.* **2022**, *12*, 134.
- [235] A. Andersson, L. Larsson, L. Stenbeck, F. Salmén, A. Ehinger, S. Z. Wu, G. Al-Eryani, D. Roden, A. Swarbrick, Å. Borg, J. Frisén, C. Engblom, J. Lundeberg, *Nat. Commun.* **2021**, *12*, 6012.
- [236] R.-Y. Ma, A. Black, B.-Z. Qian, *Trends Immunol.* **2022**, *43*, 546.
- [237] E. A. Smith, H. C. Hodges, *Trends Cancer* **2019**, *5*, 411.
- [238] X. Ren, B. Kang, Z. Zhang, *Genome Biol.* **2018**, *19*, 211.
- [239] T. Hara, R. Chanoch-Myers, N. D. Mathewson, C. Myskiw, L. Atta, L. Bussema, S. W. Eichhorn, A. C. Greenwald, G. S. Kinker, C. Rodman, L. N. Gonzalez Castro, H. Wakimoto, O. Rozenblatt-Rosen, X. Zhuang, J. Fan, T. Hunter, I. M. Verma, K. W. Wucherpfennig, A. Regev, M. L. Suvà, I. Tirosh, *Cancer Cell* **2021**, *39*, 779.
- [240] A. C. Greenwald, N. G. Darnell, R. Hoefflin, D. Simkin, C. W. Mount, L. N. Gonzalez Castro, Y. Harnik, S. Dumont, D. Hirsch, M. Nomura, T. Talpir, M. Kedmi, I. Goliand, G. Medici, J. Laffy, B. Li, V. Mangena, H. Keren-Shaul, M. Weller, Y. Addadi, M. C. Neidert, M. L. Suvà, I. Tirosh, *Cell* **2024**, *187*, 2485.
- [241] F. Chen, A. T. Wassie, A. J. Cote, A. Sinha, S. Alon, S. Asano, E. R. Daugharthy, J.-B. Chang, A. Marblestone, G. M. Church, A. Raj, E. S. Boyden, *Nat. Methods* **2016**, *13*, 679.
- [242] C. Sautès-Fridman, F. Petitprez, J. Calderaro, W. H. Fridman, *Nat. Rev. Cancer* **2019**, *19*, 307.
- [243] S. Han, D. Fu, G. W. Tushoski, L. Meng, K. M. Herremans, A. N. Riner, T. J. Geoge, Z. Huo, S. J. Hughes, *Theranostics* **2022**, *12*, 4980.
- [244] R. Moncada, D. Barkley, F. Wagner, M. Chiodin, J. C. Devlin, M. Baron, C. H. Hajdu, D. M. Simeone, I. Yanai, *Nat. Biotechnol.* **2020**, *38*, 333.
- [245] V. M. Ravi, N. Neidert, P. Will, K. Joseph, J. P. Maier, J. Kückelhaus, L. Vollmer, J. M. Goeldner, S. P. Behringer, F. Scherer, M. Boerries, M. Follo, T. Weiss, D. Delev, J. Kernbach, P. Franco, N. Schallner, C. Dierks, M. S. Carro, U. G. Hofmann, C. Fung, R. Sankowski, M. Prinz, J. Beck, H. Salié, B. Bengsch, O. Schnell, D. H. Heiland, *Nat. Commun.* **2022**, *13*, 925.
- [246] A. L. Ji, A. J. Rubin, K. Thrane, S. Jiang, D. L. Reynolds, R. M. Meyers, M. G. Guo, B. M. George, A. Mollbrink, J. Bergensträhle, L. Larsson, Y. Bai, B. Zhu, A. Bhaduri, J. M. Meyers, X. Rovira-Clavé, S. T. Hollmig, S. Z. Aasi, G. P. Nolan, J. Lundeberg, P. A. Khavari, *Cell* **2020**, *182*, 497.
- [247] S. Z. Wu, G. Al-Eryani, D. L. Roden, S. Junankar, K. Harvey, A. Andersson, A. Thennavan, C. Wang, J. R. Torpy, N. Bartonicek, T. Wang, L. Larsson, D. Kaczorowski, N. I. Weisenfeld, C. R. Uyttingco, J. G. Chew, Z. W. Bent, C.-L. Chan, V. Gnanasambandapillai, C.-A. Dutertre, L. Gluch, M. N. Hui, J. Beith, A. Parker, E. Robbins, D. Segara, C. Cooper, C. Mak, B. Chan, S. Warriar, et al., *Nat. Genet.* **2021**, *53*, 1334.
- [248] I. Dagogo-Jack, A. T. Shaw, *Nat. Rev. Clin. Oncol.* **2018**, *15*, 81.
- [249] K. Schmelz, J. Toedling, M. Huska, M. C. Cwikla, L.-M. Kruetzfeldt, J. Proba, P. F. Ambros, I. M. Ambros, S. Boral, M. Lodrini, C. Y. Chen, M. Burkert, D. Guergen, A. Szymansky, K. Astrahantseff, A. Kuenkele, K. Haase, M. Fischer, H. E. Deubzer, F. Hertwig, P. Hundsdoerfer, A. G. Henssen, R. F. Schwarz, J. H. Schulte, A. Eggert, *Nat. Commun.* **2021**, *12*, 6804.
- [250] Z. Ezzoukhy, E. Henriët, F. P. Cordelières, J.-W. Dupuy, M. Maître, N. Gay, S. Di-Tommaso, L. Mercier, J. G. Goetz, M. Peter, F. Bard, V. Moreau, A.-A. Raymond, F. Saltel, *Nat. Commun.* **2018**, *9*, 2031.
- [251] V. M. Ravi, P. Will, J. Kueckelhaus, N. Sun, K. Joseph, H. Salié, L. Vollmer, U. Kuliesiute, J. von Ehr, J. K. Benotmane, N. Neidert, M. Follo, F. Scherer, J. M. Goeldner, S. P. Behringer, P. Franco, M. Khiat, J. Zhang, U. G. Hofmann, C. Fung, F. L. Ricklefs, K. Lamszus, M. Boerries, M. Ku, J. Beck, R. Sankowski, M. Schwabenland, M. Prinz, U. Schüller, S. Killmer, et al., *Cancer Cell* **2022**, *40*, 639.
- [252] A. Comba, S. M. Faisal, P. J. Dunn, A. E. Argento, T. C. Hollon, W. N. Al-Holou, M. L. Varela, D. B. Zamlar, G. L. Quass, P. F. Apostolides, C. Abel2nd, C. E. Brown, P. E. Kish, A. Kahana, C. G. Kleer, S. Motsch, M. G. Castro, P. R. Lowenstein, *Nat. Commun.* **2022**, *13*, 3606.
- [253] T. J. Rowland, G. Dumbović, E. P. Hass, J. L. Rinn, T. R. Cech, *Proc. Natl. Acad. Sci. USA* **2019**, *116*, 18488.
- [254] J. Qi, H. Sun, Y. Zhang, Z. Wang, Z. Xun, Z. Li, X. Ding, R. Bao, L. Hong, W. Jia, F. Fang, H. Liu, L. Chen, J. Zhong, D. Zou, L. Liu, L. Han, F. Ginhoux, Y. Liu, Y. Ye, B. Su, *Nat. Commun.* **2022**, *13*, 1742.
- [255] M. V. Hunter, R. Moncada, J. M. Weiss, I. Yanai, R. M. White, *Nat. Commun.* **2021**, *12*, 6278.
- [256] Y. Liu, A. Enniful, Y. Deng, R. Fan, *bioRxiv* **2020**.
- [257] X. Sui, J. A. Lo, S. Luo, Y. He, Z. Tang, Z. Lin, Y. Zhou, W. X. Wang, J. Liu, X. Wang, *bioRxivorg* **2024**.
- [258] S. Kanatani, J. C. Kreuztmann, Y. Li, Z. West, L. L. Larsen, D. V. Nikou, I. Eidhof, A. Walton, S. Zhang, L. R. Rodríguez-Kirby, J. L. Skytte, C. G. Salinas, K. Takamatsu, X. Li, D. H. Tanaka, D. Kaczynska, K. Fukumoto, R. Karamzadeh, Y. Xiang, N. Uesaka, T. Tanabe, M. Adner, J. Hartman, A. Miyakawa, E. Sundström, G. Castelo-Branco, U. Roostalu, J. Hecksher-Sørensen, P. Uhlén, *Science* **2024**, *386*, 907.
- [259] J. Ren, H. Zhou, H. Zeng, C. K. Wang, J. Huang, X. Qiu, X. Sui, Q. Li, X. Wu, Z. Lin, J. A. Lo, K. Maher, Y. He, X. Tang, J. Lam, H. Chen, B. Li, D. E. Fisher, J. Liu, X. Wang, *Nat. Methods* **2023**, *20*, 695.
- [260] F. M. Fazal, S. Han, K. R. Parker, P. Kaewsapsak, J. Xu, A. N. Boettiger, H. Y. Chang, A. Y. Ting, *Cell* **2019**, *178*, 473.
- [261] Z. Liu, F. Guo, Y. Zhu, S. Qin, Y. Hou, H. Guo, F. Lin, P. R. Chen, X. Fan, *Nat. Commun.* **2024**, *15*, 2712.
- [262] D. Feldman, A. Singh, J. L. Schmid-Burgk, R. J. Carlson, A. Mezger, A. J. Garrity, F. Zhang, P. C. Blainey, *Cell* **2019**, *179*, 787.
- [263] J. Gu, A. Iyer, B. Wesley, A. Tagliatalata, G. Leuzzi, S. Hangai, A. Decker, R. Gu, N. Klickstein, Y. Shuai, K. Jankovic, L. Parker-Burns, Y. Jin, J. Y. Zhang, J. Hong, S. Niu, J. Chou, D. A. Landau, E. Azizi, E. M. Chan, A. Ciccia, J. T. Gaubomme, *bioRxivorg* **2023**.
- [264] L. Binan, S. Danquah, V. Valakh, B. Simonton, J. Bezney, R. Nehme, B. Cleary, S. L. Farhi, *bioRxivorg* **2023**.



Tianxiao Hui received his B.S. in 2023 from China Pharmaceutical University. Currently, he is a Ph.D. student in the Center for Life Sciences at Peking University. His research focuses on epitranscriptomics and spatial multi-omics.



Jian Zhou received his B.S. in 2023 from Nankai University. Currently, he is a Ph.D. student in the Center for Life Sciences at Tsinghua University. His research focuses on the spatial omics technologies applied in cancer biology.



Hu Zeng received his B.S. in biology sciences from Sun Yat-Sen University in 2013 and his Ph.D. in biochemistry and molecular biology from Peking University in 2019. He completed postdoctoral research at the Broad Institute of MIT and Harvard. In 2023, he joined the College of Future Technology and the Center for Life Sciences at Peking University as a tenure-track assistant professor. His research interests encompass the development of spatial omics technologies, the regulation of gene expression, and the study of neurological diseases.